Transcriptome analysis reveals infection strategies employed by *Fusarium graminearum* as a root pathogen

Yi Ding[a,c,*], Donald M Gardiner[a], Kemal Kazan[a,b,*]

[a]Agriculture and Food, Commonwealth Scientific and Industrial Research Organization, 306 Carmody Road, St Lucia, 4067, Queensland, Australia;

[b]Queensland Alliance for Agriculture and Food Innovation (QAAFI), Alliance for Agriculture and Food Innovation (QAAFI), The University of Queensland, Brisbane, St Lucia, 4067, Queensland, Australia;

[c]Current address: The Plant Breeding Institute, School of Life & Environmental Sciences, Faculty of Science, The University of Sydney, Cobbitty, 2570, New South Wales, Australia;

*Corresponding authors.

yi.ding@sydney.edu.au (Yi Ding), Kemal.kazan@csiro.au (Kemal Kazan)

Abstract

The fungal pathogen *Fusarium graminearum* infect both heads and roots of cereal crops causing several economically important diseases such as head blight, seedling blight, crown rot and root rot. Trichothecene mycotoxins such as deoxynivalenol (DON), a well-known virulence factor, produced by *F. graminearum* (*Fg*) during disease development is also an important health concern. Although how *F. graminearum* infects above-ground tissues is relatively well studied, very little is known about molecular processes employed by the pathogen during below-ground infection. Also unknown is the role of DON during root infection. In the present study, we analyzed the transcriptome of *F. graminearum* during root infection of the model cereal *Brachypodium distachyon.* We also compared our *Fg* transcriptome data during root infection with those reported during wheat head infection. These analyses suggested that both shared and unique infection strategies employed by the pathogen during colonization of different host tissues. Several metabolite biosynthesis genes

induced in *F. graminearum* during root infection could be linked to phytohormone production, implying that the pathogen likely interferes root specific defenses. In addition, to understand the role of DON in *Fg* root infection, we analyzed the transcriptome of the DON deficient *Tri5* mutant. These analyses showed that the absence of DON had a significant effect on fungal transcriptional responses. Although DON was produced in infected roots, this mycotoxin did not act as a virulence factor during root infection. Our results reveal new mechanistic insights into the below-ground strategies employed by *F. graminearum* that may benefit the development of new genetic tools to combat this important cereal pathogen.

Introduction

Fungal plant pathogens have adopted versatile strategies to colonize their hosts. While some fungal pathogens show strict host and tissue specificity, others can adjust their lifestyles to infect different hosts and tissues. Some fungal pathogens such as the rice blast *Magnaporthe oryzae* (Marcel et al., 2010; Sesma and Osbourn, 2004) and the corn smut *Ustilago maydis* (Mazaheri-Naeini et al., 2015), which commonly invade above-ground plant parts, can also undergo developmental processes resembling to root infecting fungi. Such changes in the pathogen may require sensing of host signals and we previously showed that sensing of root signals prior to root infection by *Fg* can indeed lead to developmental changes in the pathogen (Ding et al., 2020). As a member of the *Fusarium* species complex, *Fusarium graminearum* (*Fg*) causes Fusarium Head Blight (FHB) or scab, one of the most economically important diseases of cereal crops. FHB causes substantial yield losses and mycotoxin contaminations of grains, resulting in billions of dollars of economic losses worldwide and threatening our food supply and safety (Chen et al., 2019; Trail, 2009). Most studies on FHB have so far focused on wheat heads as the pathogen initially infects individual wheat florets from which it can spread to other florets through the rachis and can eventually colonize the whole spike. However, recent research has shown that *Fg* is also capable of infecting roots and young seedlings of wheat, barley and maize, causing crown rot, root rot and seedling blight (Henkes et al., 2011; Lanoue et al., 2010; Stephens et al.,

2008; Wang et al., 2015; Zhou et al., 2019). During the initiation of root infection, *Fg* forms a peg structure outside the root surface and move inter- and intra-cellularly without causing root necrosis. This early colonization stage is followed by a transition of the fungus to a necrotrophic life style where lesions develop and spread to stems and aboveground tissues (Wang et al., 2015).

The availability of the complete genome sequence of *Fg* makes investigations of global regulation of gene expression in this fungus feasible (Kazan and Gardiner, 2018a; Ma et al., 2013). Infection strategies of *Fg* evaluated by transcriptome analyses in different hosts and tissues exclusively during infection of their above-ground tissues such as heads, stems and coleoptiles revealed mostly distinct, but also common gene expression patterns (Boedi et al., 2016; Harris et al., 2016; Lysøe et al., 2011; Zhang et al., 2012, 2016). Interestingly, different cereal species can produce different defense-related metabolites (Dutartre et al., 2012) and such differences may explain why *Fg* might need to tailor its arsenal during colonization of different hosts (Harris et al., 2016). A recent comparative transcriptomic study of *Fg* also showed differential expression of fungal genes during infection of FHB resistant and susceptible wheat genotypes (Pan et al., 2018).

Although transcriptome studies have provided clues associated with host specificity of the *Fg* infection process, fungal transcriptomes of *Fg* mutants with altered virulence have rarely been tested on the same hosts. The mycotoxin deoxynivalenol (DON) is a *Fg* virulence factor during infection of wheat heads (Proctor et al., 1995). DON may also be needed during the interaction of *Fg* with its broader environment (Audenaert et al., 2013). The first step in DON biosynthesis is catalyzed by the trichodiene synthase Tri5, which cyclizes farnesyl pyrophosphate to trichodiene (Hohn and Beremand, 1989). In contrast to its strong expression pattern during wheat head infection, *Tri5* did not show increased *in planta* expression during wheat coleoptile infection, suggesting that DON's effect on pathogen virulence is tissue specific (Zhang et al., 2012). Other studies have suggested a crucial role for DON during the colonization of wheat stems by *Fg* and the related pathogens *F.*

pseudograminearum and *F. culmorum* (Desmond et al., 2008; Mudge et al., 2006; Powell et al., 2017; Scherm et al., 2013a). The recent finding where Fhb7-mediated FHB and crown rot disease resistance relies on DON detoxification also highlighted virulence function of this mycotoxin in wheat (Wang et al., 2020). Furthermore, DON is known to activate defense gene expression in wheat (Desmond et al., 2008). Indeed, host transcriptional changes observed in *Brachypodium distachyon* (*Bd*) and wheat spikelets infected by the *Tri5* deletion mutants (ΔTri5) differed from those by wildtype *Fg* (Brauer et al., 2020; Pasquet et al., 2014). DON biosynthesis in *Fg* is regulated by *Tri6* and *Tri10* transcription factors. Analyses of deletion mutants for these genes by transcriptome profiling during plant infection revealed significant transcriptional alterations for a large number of genes, many of which have not been implicated previously in toxin production (Seong et al., 2009). Genetic analyses undertaken in *Fg* have identified many genes influencing DON biosynthesis (Chen et al., 2019). However, DON-non-producing mutants have not been employed for evaluating the effect of this toxin on global transcriptional responses in *Fg*.

Phytohormones mediate immune responses in plants after pest or pathogen attack (Pieterse et al., 2009). In turn, plant pathogenic fungi have evolved ways to compromise host hormone pathways. This is achieved by degrading or producing phytohormones or interfering with their signaling pathways (Kazan and Lyons, 2014; Patkar and Naqvi, 2017). For instance, emerging evidence suggests that phytohormones such as abscisic acid (ABA), gibberellic acid (GA) and ethylene (ET) produced by fungi participate in pathogenicity (Chanclud and Morel, 2016). Previous studies indicated that *Fg* can likely produce auxin (IAA) and ET that may be utilized for attenuating host defenses during FHB (Foroud et al., 2019; Luo et al., 2016; Svoboda et al., 2019). In addition, SA hydroxylases were proposed to be involved in the degradation of host SA by *Fg* (Hao et al., 2019; Qi et al., 2019; Rocheleau et al., 2019). However, how hormonal compounds produced by *Fg* or the host plant are metabolized or involved in host infection is poorly studied. This is at least in part due to potential co-

existence of phytohormones derived from both host and the pathogen in the infected tissue and the lack of knowledge on fungal genes involved in phytohormone biosynthesis.

Currently, potential molecular mechanisms employed by *Fg* during root infection are unknown (Kazan and Gardiner, 2018a). A global transcriptome analysis would provide a powerful way to broadly reveal previously unknown features during root infection, thus promoting development of new strategies for combating this pathogen. In addition, to what extent DON may affect global transcription in the pathogen has not been investigated. We previously reported an RNA-seq based transcriptome profiling of *Fg* prior to its physical contact with *Bd* roots. This analysis enabled us to discover novel genes that are involved in nitric oxide (NO) production in *Fg* upon sensing of root signals (e.g. metabolites found in the root exudates) and pathogen virulence (Ding et al., 2020). In this study, using *Bd* as a cereal model, we asked how *Fg* behaves as a root pathogen. To answer this question, we analyzed the transcriptome of *Fg* during infection of *Bd* roots. We analyzed phytohormone levels of infected *Bd* roots to understand potential roles played by phytohormones derived from the fungus. In addition, by comparing the transcriptomes of WT *Fg* and the DON deficient *Tri5* mutant, we uncovered novel insights into global effects of DON on fungal gene expression and metabolism during the infection of host roots.

Materials and methods

Plant and fungal materials and root infection assay

The *Fg* CS3005 WT, *Tri5* mutant (Desmond et al., 2008) and *Tri5-GFP* expressing (Gardiner et al., 2009) strains were routinely maintained on Potato Dextrose Agar (PDA, BD Difco). *Bd* (Bd21-3) seeds were surface sterilized and pre-germinated on filter paper (Whatman) placed in 150mm x 25 mm petri dishes (Corning) for 5 days. *Bd* roots inoculation with the *Fg* strains was carried out as described previously (Ding et al., 2020). Briefly, agar plugs (0.25 cm diameter) taken from fungal culture plates (Carboxymethylcellulose agar) were transferred to center of minimum media (pH 7) plates and pre-grown for 3 days. Five-day-old *Bd* seedlings

were placed above the fungal colonies and inoculated for additional 5 days. Three biological replicates for *Fg* WT and ΔTri5 inoculated seedlings, and the *Fg* WT alone mycelia were produced by pooling materials from 10-12 plants or fungal mycelia.

RNAseq and transcriptomic analyses

Fungal and root materials were frozen in liquid nitrogen immediately after harvest. Total RNA was extracted from homogenized samples using a Qiagen RNeasy plant RNA extraction kit with on-column DNase I (Qiagen) digestion following manufacturer's instructions. RNA was quantified and quality-checked prior to sequencing. An Illumina HiSeq2500 High Output platform was used to generate 50-base pair single-end reads (Australian Genome Research Facility). Reads quality control, alignment, transcript abundance and differential expression (DE) analyses were performed according to the method described previously (Ding et al., 2020). For pairwise comparison (*Fg*WT-only vs. *Fg*WT-*Bd*, or *Fg*WT-*Bd* vs. ΔTri5-*Bd*), different sample files were normalized and merged. Reads were measured as FPKM (Fragments Per Kilobase of gene model per Million reads mapped), and a normalization method developed by Hart et al. (2013) was used and to eliminate background noise of FPKM values where genes with a Gaussian-fit derived $\log_2$(FPKM) value higher than -3 were considered as expressed. |log2 fold change| ≥ 1 and Benjamini and Hochberg-adjusted P value < 0.05 were applied to DE genes. RNAseq data are available at NCBI under the accession no. PRJNA631873.

Annotation and functional categorization of differentially expressed genes (DEGs)

BLAST2GO (Götz et al., 2008) was used to assign annotations for fungal DEGs. BLASTP reciprocal best hit analyses were performed in order to identify putative orthologous genes and match unique gene identifiers of the *Fg* CS3005 and PH-1 strains (Gardiner et al., 2014). Based on the PH-1 identifiers, classification ontology of DEGs from pairwise comparisons was annotated with FungiFun2 and subsequently subjected to enrichment analyses (https://elbe.hki-jena.de/fungifun). Functional categories were considered as enriched in the

158 genome if an enrichment Benjamini-Hochberg adjusted P value is smaller than 0.05.
159 Prediction of protein cellular localizations, secretome and putative effectors, transporters,
160 carbohydrate-active enzymes, lipases, secondary metabolism enzymes and transcription
161 factors was according to previously described methods (Ding et al., 2020).

162 **Identification of homologous genes between *Fg* and *Fp***

163 All RNAseq reads were mapped to the *Bd* reference genome first. Unmapped reads were
164 extracted and aligned to the *Fg* CS3005 and *Fp* CS3096 reference genomes, respectively,
165 as per previously described (Ding et al., 2020). Only reads that could be mapped to both
166 genomes were retained. Next, read counts measured as FPKM values were log transformed,
167 normalized and subjected to PCA analysis (Fig. S4). Homologous genes within *Fg* and *Fp*
168 were identified using a reciprocal best BLAST hit (RBBH) approach. Gene orthologs with
169 identity of equal or higher than 99% were kept and used for syntenic analysis using a R
170 package shinyCircos (Yu et al., 2018).

171 **cDNA synthesis and quantitative real-time PCR analysis**

172 0.5-1 µg total RNA was prepared for first-strand cDNA synthesis using the superscript IV
173 synthesis kit (Invitrogen, USA) and quantitative real-time RT-PCR (qRT-PCR) was
174 performed using the ViiA 7 real-time PCR detection platform (Applied BioSystems). Primers
175 were based on previous studies (Ding et al., 2020; Voigt et al., 2005). Expression levels
176 were normalized to the fungal house-keeping gene *α-Tubulin* and were averaged over three
177 biological replicates.

178 **Root sectioning and fluorescence microscopy**

179 Root dissection was carried out following a previous described method (Ursache et al.,
180 2018). Briefly, roots were harvested at 5dpi and fixed with 4% paraformaldehyde (Sigma) in
181 PBS buffer (pH=6.9) overnight, washed twice with PBS buffer and cleared with ClearSee
182 solution (Ursache et al., 2018) for 3 days. After clearing, roots were hand sectioned from 3

cm above the tips and stained with 0.2% Basic Fuchsin (Sigma). To image GFP and Basic Fuchsin fluorescence, root samples were observed using 488-nm excitation / 519-nm emission, and 561-nm excitation / 625-nm emission, respectively, on a Zeiss Axio Imager M2 microscopy.

UHPLC quantification of metabolites

For metabolite extractions, mock and *Fg*-infected roots, fungal mycelia and media samples were collected at 5 dpi, immediately frozen and ground in liquid nitrogen. 100 mg of fine-ground materials were resuspended in 2 mL extraction buffer (Ethyl acetate: methanol: dichloromethane, 3:2:1 v/v). 5 µL extracts from 6 replicates of each conditioned sample were injected into a Waters ACQUITY ARC UPLC system with Photodiode Array and passed through a Phenomenex Kinetex column (C18, 1.7 µm, 100 × 2.1 mm). The mobile phases consisted of solvent A (10 mM ammonium formate in water) and solvent B (10 mM ammonium formate in acetonitrile). The gradient program was a linear gradient from 2-40% solvent B delivered over 22 min followed by 40-80% B over 1.5 min at a constant flow rate of 0.4 mL per minute. As external standards, jasmonic acid (Sigma, 10 mM), methyl-jasmonate (Sigma, 40 mM), salicylic acid (Sigma, 10 mM), deoxynivalenol (Sigma, 100 ng/µL), gibberellic acid (Sigma, 10 mM), indole-3-actic acid (Sigma, 2 mM) were freshly prepared for serial dilutions (10x, 100x, 1000x, 10000x). Metabolites were quantified according to the concentration-gradient derived standard curves of external standards. Chromatography absorbance data were aligned using the following wavelengths: 204nm (for SA, JA and MeJA), 254nm (for IAA and DON) and 214nm (for GA), and extracted using the Empower 3 software (Waters).

Results and discussion

The *Fg* transcriptome during *Bd* root infection

Despite various studies investigating the transcriptome of *Fg* during colonization of above-ground tissues, *Fg* transcriptome during root infection has not been studied before (Kazan

209 and Gardiner, 2018a). Therefore, here, we first investigated the *Fg* transcriptome during root
210 infection of the model host *Bd*. This transcriptome experiment, which was initially designed
211 for the discovery of a novel host-sensing mechanism in *Fg* prior its physical contact with
212 roots, included three replicates of each of 1) *Fg* grown on minimal media (MM) (*Fg*-only) 2)
213 *Fg*WT and *Bd* roots grown together on MM without physical contact, 3) WT *Fg* colonizing *Bd*
214 roots on MM (*Fg*WT colonization) and 4) a *Tri5* mutant colonizing *Bd* roots (ΔTri5
215 colonization). Previously, by comparing 1 with 2, we discovered new regulators involved in
216 host sensing-mediated NO production (Ding et al., 2020). Here, we report on the
217 comparisons between 1 and 3, 1 and 4 and 3 and 4, as detailed analyses of these have not
218 been reported previously.

219 A total of 174,399,800 single-end reads, including 114,577,185 reads from *Fg* alone and *Fg*-
220 infected *Bd* root samples (Ding et al., 2020) and 59,822,615 reads from the ΔTri5 root
221 samples were generated by Illumina sequencing of mRNA libraries (Suppl. data 1). Prior to
222 read mapping to the *Fg* CS3005 genome (Gardiner et al., 2014), reads aligned to the *Bd*
223 genome were filtered. Of these filtered reads across all the samples, at least 91%, ranging
224 from 5 to 19.9 million, were mapped to the *Fg* reference genome. Among these mapped
225 reads, less than 0.3% matched to multiple genomic locations (Suppl. data 1). Out of the
226 12590 transcripts detected, 11942, 11291 and 11327 were found actively expressed in *Fg*-
227 only, *in* WT *Fg* colonization and in *Tri5* mutant colonization conditions, respectively.

228 Our analysis revealed a total of 2049 genes that were differentially expressed (DE) (log2 FC
229 ≥ 1 and adjusted p value < 0.05) (Fig. 1A, Suppl. data 2) during colonization of *Bd* roots
230 relative to *Fg*-only. Of these, 1281 and 768 were up- and down-regulated, respectively,
231 during root colonization. The proportion of DE genes (DEGs) (around 20% of total number of
232 genes found in the *Fg* genome) was similar to those observed during above-ground infection
233 by *Fg* in other studies (Brown et al., 2017; Puri et al., 2016). A previous study indicated that
234 some defense genes are similarly regulated in wheat roots and spikes in response to *Fg* (Q.
235 Wang et al., 2018), suggesting that common strategies might be employed by *Fg* to infect

different tissue types. Indeed, we previously reported that fungal knockouts of several DEGs identified here showed defects in both root and head infection (Ding et al., 2020).

Fungal processes employed by *Fg* during root infection

Detailed analysis of DEGs (*Fg*-only *vs* WT *Fg* colonization) revealed a number of enriched functional categories likely to be used by the pathogen during root infection. Below, some of these functional categories were discussed in more detail.

Genes encoding plant cell wall degrading enzymes (CWDE)

The *Fg* genome comprises a large number of genes encoding hydrolytic enzymes, transporters, secreted proteins and multiple gene clusters associated with secondary metabolite biosynthesis (Scherm et al., 2013; Sieber et al., 2014). These enzymes, non-enzymatic proteins and secondary metabolites together are generally considered fungal pathogenicity factors and their deployment during *Bd* root colonization indicates the importance of these pathway for sustaining the infection process. Indeed, over 30% of DEGs encode secondary metabolism enzymes (SMEs), secreted proteins, carbohydrate-active enzymes (CAZymes) and transporters (Fig. 1A). The most enriched categories for significantly up-regulated genes were associated with carbohydrate hydrolytic pathways (Suppl. data 3). Functional annotations showed that over half of the *in planta* activated CAZymes displayed modular structures related to CWDE acting on wall polymers such as cellulose, hemicellulose, lignin and pectin (Fig. 1B, Suppl. data 4), indicating the utilization of carbon from plant cell walls is a prominent capability of *Fg* during the colonization of *Bd* roots.

Genes encoding secreted proteins and putative effectors

Fungal pathogens produce many small secreted proteins or effectors to help facilitate host colonization. However, relatively little is known about potential *Fg* effectors. By comparing our DEGs with the previously defined *Fg* secretome (Brown et al., 2012) and using the EffectorP 2.0 software (Sperschneider et al., 2018), we identified 250 putative secreted proteins along with 65 predicted fungal effector encoding genes (Fig S1C, Suppl. data 4 and

5). Many of these secreted protein genes, including 189 induced ones (Suppl. data 5), encode putative lipases and peptidases predicted to perform hydrolytic functions (Fig. 1C). Among the 65 predicted effector-encoding genes, 52 were significantly up-regulated during *Bd* root infection (Suppl. data 5). Some of these DE genes were reported to encode effectors actively secreted by *Fg* during *in vitro* growth. For example, *FG05_04074* encodes a protein of unknown function detected in two different secretomes (Lu and Edwards, 2016; Yang et al., 2012). Other putative effectors with annotated functional domains also found in previous studies included two glycoside hydrolases (FG05_11037 and FG05_06466), a putative acetylesterase (FG05_11280), a putative endonuclease (FG05_03365) and a cerato-platanin family protein (FG05_10212) for which roles of protection against host defense have been proposed (Lu and Edwards, 2016; Quarantin et al., 2016; Yang et al., 2012). Interestingly, the top induced effector candidates were mostly with predicted enzymatic functions (Suppl. data 5). Function of these differentially regulated putative effectors, such as FG05_04735 encoding a putative hypersensitive response-inducing elicitor and FG05_02255 a LysM domain containing protein (Suppl. data 5), could be predicted in comparison with those containing similar structural domains from different fungal pathogens and generally associated with host penetration, spore dispersal, triggering plant defense responses, inhibiting chitin-induced immunity or protecting against plant lysis (De Jonge et al., 2010; Khan et al., 2016; Lo Presti et al., 2015; Marshall et al., 2011; Mentlak et al., 2012). Although exact functions of these genes up-regulated during infection are largely unknown, it can be speculated that these secreted proteins and putative effectors could benefit the fungus during the colonization of host roots.

Genes encoding secondary metabolism enzymes (SME)

Fg is known to produce many secondary metabolites (SMs) during infection (Ma et al., 2013). In line with this, a strong induction of expression could be observed for genes encoding key signature enzymes (Fig. S1A), including the longiborneol synthase CLM1 (FG05_10397), butenolide synthase (FG05_08079), TRI5 and the terpenoid synthase DTC1 (FG05_03066)

289 during infection (Suppl. data 6), suggesting that the corresponding products culmorin,
290 butenolide, trichothecene and carotenoid may be the major mycotoxins delivered by the
291 fungus to facilitate root infection. Among them, butenolide and trichothecene pathways are
292 known to be co-regulated *in vitro* and *in planta* (Sieber et al., 2014). In contrast, down-
293 regulation or very low *in planta* expression of other key SME genes, such as *PKS12*, *NPS2*,
294 *NPS1*, *PKS4* and *PKS10* (Suppl. data 6), indicates that certain types of mycotoxins such as
295 aurofusarin, ferricrocin, malonichrome, zearalenone and fusarin C might not be highly
296 produced by *Fg* during root colonization. Aurofusarin does not affect wheat head infection by
297 *Fg* (Malz et al., 2005), whereas ferricrocin and malonichrome have been shown to be
298 important for pathogenesis-related development of *Fg* (Oide et al., 2014). The tailoring
299 enzyme genes are usually clustered and co-regulated with the corresponding signature
300 enzyme genes in *Fg*. These genes encode cytochrome P450s, oxidoreductases,
301 acyltransferases and methyltransferases mainly involved in the SM pathway responsible for
302 biosynthesis and modification of SM products (Sieber et al., 2014). Therefore, up-regulation
303 of a large portion of tailoring enzyme genes found in this study is consistent with the
304 regulation pattern of the signature enzymes (Fig. S1B).

305 **Genes encoding fungal transporters**

306 Transporter encoding genes mostly induced during *Bd* root colonization comprised a large
307 group within the DE gene list (Fig. S1C, Suppl. data 7). Indeed, the regulation of transporter
308 genes, particularly those associated with carbohydrate and nitrogen uptake as well as the
309 ATP-binding cassette transporters (ABC transporters), is often linked to fungal nutrient
310 assimilation, sensing, defense and pathogenicity status in pathogenic fungi (Abou Ammar et
311 al., 2013; Coleman and Mylonakis, 2009; Divon and Fluhr, 2007; Gardiner et al., 2013;
312 Schuler et al., 2015; Struck, 2015; Yin et al., 2018). Interestingly, the major facilitator
313 superfamily (MFS) transporters associated with phosphate (Pi) transport and multidrug
314 resistance (MDR) were mostly down-regulated during root infection compared to media
315 alone controls (Fig. S1C, Suppl. data 7). During colonization of maize stalk, *Fg* overcomes Pi

316 limitation by up-regulating high-affinity Pi transporter genes *FGSG_03172* and *FGSG_02426*
317 (Zhang et al., 2016). The observation here that expressions of these genes during *Bd* root
318 infection significantly reduced indicates a relatively rich root Pi environment under the
319 experimental conditions and the time point examined. The down-regulation of MDR
320 transporter genes suggested that they are possibly not essential for *Fg* to resist against root-
321 derived anti-fungal compounds or self-derived toxins. The elevated expression of a large
322 number of MFS-type carbohydrate transport genes together with the induction of PCWDE
323 genes indicate that *Fg* preferentially utilizes carbon to accomplish the infection cycle and a
324 state of glucose depletion may exist at the examined stage. The top induced ABC
325 transporters (Suppl. data 7) exclusively belonging to the ABC-G type transporters are known
326 to be associated with self-protection, possibly by effluxing of antifungal compounds in many
327 pathogenic fungi (Coleman and Mylonakis, 2009). Thus, it is likely that these ABC
328 transporters together with the MFS family multidrug resistance transporters could contribute
329 to the virulence and fitness of *Fg* by detoxifying plant defense compounds.

330 We also observed that genes encoding amino acid-related transporters such as the amino
331 acid/polyamine/organocation (APC) family and the amino acid/auxin permease (AAAP)
332 family transporters, which are the major nitrogen transporters, were differentially expressed
333 during root infection. In contrast, no inorganic nitrogen transporter gene showed altered
334 expression (Suppl. data 7). This suggests that *Fg* root infection requires plant-derived
335 organic nitrogen sources, and is consistent with the finding that polyamines as well as their
336 amino acid precursors are potent DON inducers in *Fg* and play important roles during head
337 infection (Gardiner et al., 2010, 2009). Interestingly, the highest induced transporter
338 (*FG05_02278*, over 10-fold logFC) gene encodes a putative APC family protein transporter
339 involved in choline uptake. Choline was identified as one of the major fungal growth
340 stimulators in wheat anthers and implicated in promoting *Fg* virulence (Strange et al., 1972).
341 Thus, it is possible that choline, in addition to amino acids and their derivatives, is another
342 major factor contributing to *Fg* root colonization.

A small set of 'core' genes is activated during infection of different hosts and tissues by *Fg*

To obtain additional insights into *Fg* pathogenicity, we compared the *Fg* genes found to be induced during root colonization in this study with those previously reported to be induced during the colonization of other hosts or tissues (Brown et al., 2017; Harris et al., 2016; Lysøe et al., 2011; Zhang et al., 2012, 2016). These previous studies have reported several subsets of *in-planta* expressed *Fg* genes at multiple infection time-points and different disease development stages. To make a broader comparison, *Fg* genes that were commonly induced during infection at any of the studied time-points were selected. These included 3591 *Fg* genes induced during the infection of wheat heads (Brown et al 2017), 5061 genes expressed during the infection of wheat and barley heads and maize ears (Harris et al 2016) as well as 344 and 3066 genes induced during the infection of wheat juvenile coleoptiles (Zhang et al., 2012) and maize stalks (Zhang et al., 2016), respectively (Suppl. data 8). Through these comparisons, a total of 38 *Fg* genes commonly induced across all gene lists were identified (Fig. 2A, Suppl. data 9). Some of these genes were also differentially expressed between a FHB resistant and a susceptible wheat genotype (Pan et al., 2018). Unexpectedly, no mycotoxin- or pathogenicity-related SME genes were present among these 38 genes (Fig. 2B). An ABC transporter gene, *FG05_04580* (*FgABC1*), and its flanking neighbor *FG05_04581*, which encodes a transcription factor highly inducible by the mycotoxin zearalenone (Lee et al., 2010), were found among these common genes. Deletion of *FgABC1* causes reduced virulence of *Fg* on tested wheat tissues (Abou Ammar et al., 2013; Gardiner et al., 2013). Interestingly, *FgABC1* and *FG05_04581* homologs in the closely related pathogen *F. culmorum* were both highly induced by the antifungal compound tebuconazole (Hellin et al., 2018). This indicates that FgABC1 and FG05_04581 could be involved in self-protection against various defensive chemicals consistent with the observation that FgABC1 contributes to protection against the fungicide benalaxyl (Gardiner et al., 2013). Furthermore, most of these common genes encode non-SM enzymes such as

CAZymes, peptidases and putative effectors. Among them, *FG05_03624*, a gene encoding a secreted xylanase, was previously shown to promote necrosis during *Fg* head infection (Moscetti et al., 2015). Protein homologs of several of these genes were also shown to be virulence factors in other fungal pathogens. For instance, FG05_00028 is homologous to metallopeptidases (MEP1), which were shown to be apoplastic effectors in *F. oxysporum* and *M. oryzae* (Jashni et al., 2015; Yan and Talbot, 2016). In *F. oxysporum*, the metallopeptidase FoMEP1 and the serine protease FoSEP1 act synergistically to cleave host chitinases and prevent their degradation of fungal cell walls (Jashni et al., 2015). Indeed, a serine-type proteinase inhibitor encoded by *FG05_08012* found in our gene list, shows high similarity to FoSEP1 (Suppl. data 9). Another putative hypersensitive inducing elicitor FG05_04741 shows significant homology to the *Verticillium dahlia* effector PevD1, which was shown to be a secreted elicitor triggering host defense and cell death (Liang et al., 2018). We hypothesize that these putative *Fg* effectors may perform roles that are similar to those found in other fungal pathogens. Taken together, it can be hypothesized that a common set of *Fg* genes seems to play essential roles in *Fg* for successful colonization of different tissue types.

***Fg* genes specifically upregulated in *Bd* roots**

We have identified 257 *Fg* genes that were exclusively upregulated during *Bd* root infections (Fig. 2A). Functional category analysis showed a significant enrichment for genes involved in transmembrane transport and cellular import (FDR = 0.00334). Of 34 transporter encoding genes induced, 12 were predicted to be associated with carbon transport (Suppl. data 10). This supports the finding discussed above that carbon utilization by *Fg* plays a role during *Bd* root colonization. Three ABC-G and two MDR transporters (Suppl. data 10) found among the enriched transporters might be specifically associated with detoxification of *Bd* root defense compounds. Among the four predicted effectors induced in roots (Suppl. data 10), the putative host-necrosis inducer protein FG05_10212 was shown to be constitutively expressed during infections of wheat heads and *in vitro* and confirmed as an extracellular

protein (Lu and Edwards, 2016). The induction of this effector might contribute to necrosis observed in the infected *Bd* roots. Notably, of the seven putative *Fg* PCWDEs whose transcripts were only induced in *Bd* roots, five use lignin as substrate (Suppl. data 10), suggesting that lignin-degradation by *Fg* in *Bd* roots. Overall, while some common infection strategies may be employed by *Fg* during infection of different hosts and tissue types, there appears to be also unique processes used based on the activation of specific *Fg* genes during root colonization.

Partially shared infection strategies may be used by *Fg* and its sister species *Fp* during above- and below-ground infection of *Bd*

Previously, above-ground responses to the infection of *Bd* seedlings by *F. pseudograminearum* (*Fp*), another fungal species that is highly similar to *Fg* at the whole genome level (Gardiner et al., 2018) and was previously considered to be the same species as *Fg* (Kazan and Gardiner, 2018b), have been investigated (Powell et al., 2017). Both *Fg* and *Fp* show highly similar infection patterns on *Bd* (Fitzgerald et al., 2015). In addition, most genes are located in similar genomic regions in both fungi, whereas only a few species-specific genes, which could not be revealed by syntenic analysis, were found in genomic locations displaying high SNP densities (Gardiner et al., 2018). To further explore organ specificity of *Fg* infection on the same host, we compared the transcriptome of *Fg* with that of *Fp* (NCBI accession no. SRR3695327), during above ground infection of *Bd* at the same time point. Only *Fg* and *Fp* orthologous genes, which could be mapped to both of the genomes and share an identity of ≥99% were retained in this comparison. This stringent cut-off allows comparisons of only highly conserved genes that might be predicted to show similar pattern in expression and function in these two closely related fungal species.

In total, 1835 of the *Fg* DEGs were matched to *Fp* and formed a syntenic map (Fig. 3A and Suppl. data 11) consistent with the previously revealed genome structures (Gardiner et al., 2018). These genes were, in general, similarly expressed in *Fg* and *Fp* as indicated by the logarithmic transformed FPKM values (Fig. 3A). However, some variability in gene

expression between the two species could be observed, particularly for genes found on chromosome 2 where the *Fg* orthologs tend to be preferentially expressed, as reflected by the expression heat map (Fig. 3A). Parts of chromosome 2 were previously identified as regions of the *Fg* genome that are rapidly evolving (Sperschneider et al., 2015). By manual curation, we selected and annotated the top 20 variant genes (Fig. 3B) that included three MFS-type transporter genes and an acetate permease homolog as well as several putative defense associated genes encoding a cell-wall glycoprotein (FG05_03352), peptidases (FG05_08075 and FG05_08141), and glucosidases (FG05_03387 and FG05_08265). A Zn_2Cys_6 transcription factor (FG05_03727), which shares the highest similarity to the yeast multidrug and oxidative stress resistance regulator STB5 (Larochelle et al., 2006), was identified. Accordingly, we found several oxidative stress responsive genes encoding a molybdopterin oxidoreductase (FG05_02880), NADH-flavin oxidoreductase (FG05_08077) and a putative flavohemoglobin (FG05_04458). Notably, *FG05_03914* encoding a putative isochorismatase (ISC) gene was only expressed in *Fg* during infection of *Bd* roots. ISC-like effectors in filamentous pathogens are conserved virulence factors that can subvert plant salicylic acid (SA) pathway and interfere with host immunity (Liu et al., 2014). Resistance to biotrophic and hemi-biotrophic pathogens is usually conferred by the host SA pathway (Pieterse et al., 2012), and therefore, ISCs might be employed by *Fg* to support its hemi-biotrophic lifestyle to attenuate SA produced by the roots. The absence of *Fp ISC* transcription is consistent with the observation that host SA levels were not elevated in *Bd* plants at the early stages of infection (Powell et al., 2017). Host plants may activate tissue-specific defense signaling in response to below- and above-ground attacks (Lyons et al., 2015). To manipulate such defense responses, a fungal pathogen must evolve to a high flexibility for successful infection progressed in different host tissues. Despite the use of two fungal species, the data provided here may suggest shared infection strategies, including the interference with host defense, employed by *Fg* to support its belowground colonization.

DON influences different fungal processes in *Fg* during *Bd* root infection

The trichothecene mycotoxin DON has been shown to significantly inhibit *Bd* root growth (Pasquet et al., 2016). However, to the best of our knowledge, there has not been any study examining the effect of DON on different fungal processes in *Fg*. Therefore, we conducted an RNA-seq analysis by infecting *Bd* roots with DON producing and deficient strains to determine *Fg* genes whose expressions are modulated by DON. We first focused on genes up-regulated in the DON deficient ΔTri5 mutant strain relative to WT. Of 973 genes differentially expressed between ΔTri5 and WT, 432 genes were expressed at higher levels in ΔTri5 (Fig. 4A, Suppl. data 12). These genes were subjected to functional enrichment analysis based on the MIPS FGDB (*Fusarium graminearum* Genome Database Functional Catalogue classification) (Güldener et al., 2006). This analysis showed that these genes are enriched for transport (FDR = 0.0016) of carbon-compounds, carbohydrates, and heavy metal ions, disease, virulence and defense (FDR = 0.005) and homeostasis of phosphate (FDR = 0.02). A relatively smaller portion of fungal pathogenicity and metabolism associated genes encoding CAZymes, SMEs, transporters and secreted proteins were induced in ΔTri5 relative to WT (Fig. 4B-C, Fig. S2 and suppl. data 12-13). Only metabolic pathway genes encoding methyl- and glycol-transferases as well as phosphate, lipid and polyamine transporters were preferentially induced (Fig. S2). Host-derived phosphates, lipids as well as polyamines may influence *Fg* infection in multiple host tissue types (Gardiner et al., 2010; Zhang et al., 2016). Their enhancement might be due to a positive feedback to the lack of DON to balance the fungal metabolism and cell structure in root proliferation. In addition, 28 CAZyme encoding genes were expressed higher in ΔTri5 than in WT and many of these were putative PCWDEs involved in lignin degradation (Fig. 4B). Lignin is one of the major barriers against fungal pathogens (Bhuiyan et al., 2009). Defense related or unrelated lignin content at fungal penetration sites might affect *Fg* intra-cellular progression (Zhang et al., 2016). In wheat roots, *Fg* colonization could be observed in lignin-rich vascular bundles (Bhandari et al., 2018; Wang et al., 2015). Therefore, the upregulation of lignin-degrading enzymes in ΔTri5 could be beneficial to the fungus to compensate DON deficiency and assist root colonization. In line with this, we observed reduced lignin deposition in roots

479 colonized by ΔTri5 relative to the roots either mock-inoculated or colonized by WT *Fg* (Fig.
480 5).

481 Seven of the 33 secreted protein genes induced in ΔTri5, including a pathogenesis-related
482 protein 1 (PR1) homolog (FG05_03109) and a putative cutinase (FG05_03457), may be
483 considered putative effectors. The most differentially regulated SME genes in ΔTri5 were
484 tailoring enzyme genes encoding cytochrome P450s and oxidoreductases (Fig. S2A and
485 S2B). Surprisingly, most DEGs with elevated transcripts levels in ΔTri5 during root
486 colonization (405 out of 432 genes) were expressed either significantly lower in WT during
487 *Bd* root infection than *Fg* only or remained unchanged comparing to WT *in vitro* (Suppl. data
488 12). Besides, we noticed that none of the above-mentioned core genes was reduced in ΔTri5
489 during infection, supporting the notion that these genes may contribute to infection more
490 than others, independently of fungal DON production.

491 We next looked at the 541 significantly downregulated genes in ΔTri5 relative to WT in roots.
492 The most enriched functional categories during root infection were C-compound and
493 carbohydrate metabolism (80 genes, FDR = 0.00008), disease, virulence and defense (16
494 genes, FDR = 0.01), secondary metabolism (27 genes, FDR = 0.01), protein or peptide
495 degradation (26 genes, FDR = 0.01) and transport facilities (42 genes, FDR = 0.03) (Suppl.
496 data 14). In addition, we found two sets of adjacent genes *FG05_02297-FG05_02309* and
497 *FG05_08077-FG05_08084* that showed reduced expression in ΔTri5. Of these two sets, the
498 latter genes, which are part of the mycotoxin butanolide cluster, shared similar regulation
499 pattern with the *Tri (tricothecene)* cluster genes during infection of wheat heads (Boedi et al.,
500 2016). In the saprophytic fungus *Trichoderma arundinaceum*, the loss of trichothecene
501 production likely contributed to an increase of fungal secondary metabolites (Lindo et al.,
502 2019, 2018). Therefore, DON seems to affect fungal metabolism during *Fg* infection in *Bd*
503 roots.

504 Previously, *Tri5* deletion was reported to lead to observable metabolic changes in *Fg*
505 growing in rich medium, suggesting that DON might be linked to fungal physiology and

development (Chen et al. 2011). In line with this, we also found that several differentially regulated TF genes in ΔTri5 during root infection were putative development-associated regulatory genes (Suppl. data 15). For example, FG05_08892 (MAT1-1-1) and FG05_05151 are known to be associated with sexual development (Kim et al., 2015), FG05_01139 (FgCBF1) is a predicted chromatin remodeling regulator (Guo et al., 2016), and FG05_03597 is homologous to *Aspergillus nidulans* FlbA, which is required for the control of mycelial proliferation and activation of asexual sporulation (Yu et al., 1996). However, when grown on MM, *Tri5* was barely expressed *in vitro*, and no DON could be detected by metabolic analysis (Fig. 6D). ΔTri5 also did not show any growth defects (Chen et al., 2011). Together, our results suggest that ΔTri5 may colonize the roots by utilizing a small set of genes not used by the WT fungus.

DON is produced during *Bd* root colonization but does not act as a virulence factor

DON is a virulence factor during infection of wheat heads by *Fg* (Wang et al., 2020). However, it is unknown if this mycotoxin could also act as a virulence factor during infection of *Bd* roots. To determine this, the infection process was monitored using a *Fg* strain expressing Tri5-GFP fusion driving by the native *Tri5* gene promoter (Gardiner et al., 2009). Strong GFP signals could be visualized two days post-inoculation (dpi) in inoculated roots, indicating that the infection was progressing, and DON production was initiated (Fig. 7A and 7B). Consistent with this observation, *Tri5* was highly induced at 2 dpi and remained at high levels at later time points (3, 5, and 7 dpi) in the WT isolate (Fig. 7C). Previously, a temporarily similar infection pattern by *Fg* was also observed in wheat seedling roots (Wang et al., 2015). *Fg* root infection of wheat triggers induction of systemic defense responses in above-ground parts of the plant (Wang et al., 2018). In addition, DON preferentially inhibits root growth in wheat, *Bd* and Arabidopsis plants (Gatti et al., 2019; Masuda et al., 2007; Pasquet et al., 2016), and has been proposed to act as a major virulence factor in the early stages of *Fg* root infection (Wang et al. 2018). To assess the role of DON during root infection, a *Fg Tri5* mutant was used in inoculation experiments together with WT and Tri5-

533 GFP strains. *Bd* roots infected by ΔTri5 exhibited levels of lesion development that were like
534 those caused by WT and Tri5-GFP at 7 dpi (Fig. 7D). Therefore, while DON is a virulence
535 factor in *Fg* during FHB of wheat and is highly induced in roots, *Bd* root infection by *Fg*
536 seems to be independent of DON production. Indeed, various phytopathogenic phenotypes
537 have been described for *Fg* DON deficient mutants (Boenisch and Schäfer, 2011; Cuzick et
538 al., 2008; Jansen et al., 2005). For instance, altered levels of DON have been shown to
539 inhibit plant apoptosis-like programmed cell death (PCD) induced by heat stress in
540 Arabidopsis (Diamond et al., 2013).

541 **Phytohormone dynamics during *Fg* colonization of *Bd* roots**

542 It is becoming increasingly evident that plant pathogens interfere with phytohormone
543 pathways by producing plant hormones (Kazan and Lyons, 2014). However, pathogen-
544 produced phytohormones have rarely been examined during root infections. We therefore
545 next examined the transcriptome of *Fg* during *Bd* root infection, coupled with metabolic
546 analyses, to determine putative phytohormone associated genes in *Fg* and their potential
547 involvement in *Bd* root colonization.

548 **JA produced by *Fg* is not associated with *Bd* root colonization**

549 The oxylipin hormone jasmonic acid and its derived metabolites collectively known as
550 jasmonates (JAs) are derived from lipid peroxidation and can affect both host and fungal
551 physiological processes (Tsitsigiannis and Keller, 2007). Fungal oxylipin biosynthesis is
552 catalyzed by lipoxygenases (LOXs) (Fischer and Keller, 2016). In *F. oxysporum*, FoxLOX
553 was found to exhibit a multifunctional activity in oxylipins production, thus proposed to
554 possess a function in JA pathways (Brodhun et al., 2013). Interestingly, we noticed that the
555 *Fg* homolog of FoxLOX, *FG05_05046*, was expressed during *in vitro* growth, and highly
556 induced during root infection (4.8 fold, Table S1). JA-regulated defenses in plants can be
557 interrupted by pathogen-derived hormone analogs (Caarls et al., 2017; Patkar and Naqvi,
558 2017). The *Fg* genome does not contain a homolog of the *M. oryzae antibiotic biosynthesis*

559 *monooxygenase* (*Abm*), which converts host-derived JA into 12-hydroxyjasmonic acid
560 (12OH-JA), thus attenuating rice blast disease resistance (Patkar and Naqvi, 2017). The
561 Arabidopsis 2OG oxygenases (JOXs) are responsible for JA hydroxylation (Caarls et al.,
562 2017; Smirnova et al., 2017). We identified ten homologous of Arabidopsis JOXs in *Fg*
563 (Table S1). Of these, *FG05_08081* and *FG05_02301*, whose protein products share 22-26%
564 identity to JOXs, were induced by 8.3 and 3.9 fold, respectively, during root infection.
565 *FG05_08081* is present in the butanolide biosynthesis gene cluster, members of which were
566 also significantly upregulated during root infection (Suppl. data 2). However, whether
567 FG05_08081 and FG05_02301 are involved in JA degradation requires further analyses.

568 JA-associated host defense against *Fg* has been studied during FHB development. Inhibition
569 of JA by DON at the bottom of wheat florets promotes fungal progression through rachis
570 notes (Bönnighausen et al., 2019). Furthermore, late activation of JA signaling during FHB
571 has been proposed to correlate with a necrotrophic transition of *Fg* (Ding et al., 2011). To
572 determine if JA levels change during root infection, we quantified JA levels in *Bd* roots either
573 mock-treated or inoculated with WT *Fg* or ΔTri5 strains by high performance liquid
574 chromatography (HPLC). We found that 5 ng/mg dried material of JA was produced in *Fg*
575 mycelia grown on MM (Fig. 6A). However, JA levels found in infected and control roots were
576 much lower than 5 ng/mg and did not display any significant difference (Fig. 6A).
577 Interestingly, however, higher levels of JA derivative methyl-JA (MeJA) were detectable in
578 the roots infected by ΔTri5 than those infected by WT (Fig. 6B). Thus, DON seems to inhibit
579 MeJA production in the infected *Bd* roots. This is consistent with the observation in wheat
580 heads where MeJA levels in the ΔTri5-infected tissue were less than those infected with WT
581 *Fg* (Bönnighausen et al., 2019).

582 **SA may synergistically interact with *Bd* root defense-related metabolic pathways**

583 SA is a major defense hormone typically associated with plant defense against biotrophic
584 pathogens (Glazebrook, 2005). JA and SA accumulate at different basal levels in various
585 wheat cultivars and antagonistically fine-tune host defense responses (Powell et al., 2017).

586 Therefore, we next focused on *Fg* responses to SA. Although the SA-pathway may be
587 involved in host basal resistance against *Fg* (Ding et al., 2011; Makandar et al., 2010), SA-
588 associated systemic acquired resistance (SAR) played no role in FHB resistance (Li and
589 Yen, 2008). During infection of *Bd* seedlings by *Fp*, SA biosynthesis was induced (Powell et
590 al., 2017). However, the function of SA during root infection by *Fg* remains elusive.

591 In Arabidopsis, SA biosynthesis during pathogen infection mainly relies on the intermediate
592 chorismate processed by isochorismate synthase I (ICS1), the GH3 acyl adenylase-family
593 enzyme PBS3, and the BAHD acyltransferase-family protein EPS1 (Torrens-Spence et al.,
594 2019). The phenylalanine ammonia lyase (PAL) pathway also mediates SA synthesis
595 through the conversion of benzoic acid or coumaric acid, but only contributes to a small
596 portion of total SA production (Wildermuth et al., 2002). Similarly, some bacteria can directly
597 convert isochorismate to SA by isochorismate pyruvate lyase (IPL) (Serino et al., 1995).
598 While the host is believed to be the source of SA production in various plant-bacteria
599 interactions, whether there is a fungal origin of SA remains unknown. In the *Fg* genome, we
600 found two ICS1 homologs FG05_05195 and FG05_12934. Of these, *FG05_05195* was lowly
601 expressed (FPKM < 0.5), but *FG05_12934* exhibited constitutive and high transcript levels
602 during both *in vitro* growth and infection of *Bd* roots (Table S1). *Fg* also has an *EPS1*
603 homolog, *FG05_00237*, which was significantly upregulated during *Bd* root infection (Table
604 S1). *FG05_09331* encodes a protein sharing about 50% identity with PAL. *FG05_09331*
605 expression decreased by 2.2-fold in infected roots relative to *Fg* grown *in vitro*. No PBS3 and
606 IPL homologs could be identified in *Fg*. While expression patterns of *ICS1* and *EPS1*
607 homologs may coincide with observed SA production by *Fg*, the absence of a *PBS3*
608 homolog indicates other components or pathways could be involved in the SA biosynthesis.
609 To determine if SA is produced in *Fg-Bd* interactions, we extracted metabolites from *Bd*
610 roots with or without *Fg* inoculation and quantified SA levels by HPLC. In *Fg* mycelia, there
611 was also about 0.01 µg SA per mg dry material (Fig. 6C). Most SA was found in the roots
612 inoculated with WT *Fg*, followed by uninfected roots and the lowest levels in the ΔTri5

613 infected roots (Fig. 6C), indicating a potential role for DON in regulating SA levels during root
614 infection by *Fg* although it is difficult to estimate the exact contribution of *Bd* or *Fg* to the SA
615 levels measured.

616 SA has a direct effect on *Fg* growth, most likely associated with active degradation of SA by
617 fungal hydroxylases. In recent studies (Hao et al., 2019; Qi et al., 2019; Rocheleau et al.,
618 2019), two proteins FGSG_08116 and FGSG_03657 have been characterized with a
619 function in SA degradation. While transcription of both FGSG_08116 and FGSG_03657 can
620 be induced by external SA, fungal virulence in wheat heads was only influenced by deletion
621 of the former. The function of FGSG_03657 for SA degradation was not disabled in deletion
622 mutants. Interestingly, *FG05_03657* (a.k.a. FGSG_03657) was exclusively induced during
623 *Bd* root infection (Suppl. data 10), suggesting that it may have a role in regulating SA levels
624 in infected roots.

625 To determine if *Fg* could possess additional putative SA hydroxylase genes (Hao et al.,
626 2019), we searched the *Fg* genome and identified 28 homologs of the SA sensor and
627 degradation protein Shy1 from *Ustilago maydis* with FgShyC displaying at least 20% identity
628 to Shy1 (e-value < 10^{-5}) (Fig. S3). This similarity is much higher than the values reported
629 previously (Hao et al., 2019; Rabe et al., 2013), where the expansion of these putative
630 proteins in *Fg* was supported by phylogenetic analysis (Fig. 8A). In our current transcriptome,
631 *FG05_03657* and additional ten genes encoding putative SA hydroxylases were significantly
632 upregulated in *Fg* during root infection (Fig. 8B). Therefore, SA biosynthesis by the pathogen
633 as well as the host can contribute to the expression and regulation of these genes.

634 **Expression of genes involved in the biosynthesis of other phytohormones in *Fg***
635 **during *Bd* roots infection**

636 In addition to JA and SA, other phytohormones such as gibberellins (GAs), auxins (IAAs),
637 ethylene (ET), cytokinins (CKs) and abscisic acid (ABA) also participate in modulating host
638 defense signaling (Pieterse et al., 2012). GAs can be synthesized by a number of *Fusarium*

639 species but not by *Fg* due to the lack of a corresponding biosynthesis gene cluster (Cuomo
640 et al., 2007). As a virulence factor, GA is restricted to the necrotrophic fungal pathogen *F.*
641 *fujikuroi* (Wiemann et al., 2013) and is possibly involved in attenuating host JA signaling
642 (Navarro et al., 2008). Under our inoculation conditions, GA was detected in the roots
643 infected by WT *Fg* but not by the ΔTri5 mutant (Fig. 6F), indicating an endogenous GA
644 production in *Bd* roots upon *Fg* infection and a potential positive effect of DON on root GA
645 production. Similarly, GA accumulates in wheat heads infected by *Fg* (Bönnighausen et al.,
646 2019), thus *Fg* seems to trigger a GA-dependent response in host roots that is similar to one
647 observed in wheat florets (Buhrow et al., 2016). However, the association between DON
648 and GA production requires further investigations.

649 Fungal genes encoding indole-3-acetaldehyde dehydrogenases (Iad) and tryptophan
650 aminotransferases (IaaM) were thought to be responsible for IAA production (Reineke et al.,
651 2008). A possible third pathway for auxin biosynthesis could be mediated by *Fg* genes
652 homologous to YUCCA, a key enzyme involved in plant auxin biosynthesis (Mano and
653 Nemoto, 2012). Interestingly, only one of the three *Fg Iad* gene homologs, *FG05_02773,*
654 showed more than 4-fold induction in *Fg* during root infection as compared to *Fg* grown *in*
655 *vitro* (Table S1). In contrast, two *IaaM* homologs and a *YUCCA* homolog were significantly
656 downregulated in *Fg* inoculated roots (Table S1). Thus, the strong induction of *FG05_02773*
657 might coincide with the production of the auxin indole-3-acetic acid (IAA) by *Fg*, which could
658 thereafter compromise the host auxin pathway. Fungal auxin biosynthesis plays a role in
659 pathogenicity of several pathogens (Chanclud and Morel, 2016). In *Fg*, auxin was proposed
660 to be a virulence factor (Svoboda et al., 2019). Indeed, *Fg* is able to synthesize IAA but also
661 sensitive to exogenous application of IAA and its biosynthetic intermediates (Qi et al., 2016).
662 However, *Fg* infection strongly inhibited IAA levels in roots infected by *Fg* WT or ΔTri5 (Fig.
663 6E). This is contradictory to the findings in wheat where auxin levels increased during FHB
664 (Wang et al., 2018). Factors such as host tissue types and hormone antagonists (Kazan and
665 Manners, 2009) might be responsible for such differences.

Fg can exploit host ET signaling during colonization of both dicotyledonous and monocotyledonous plants and is believed to be capable of producing ET to counteract host defense pathways (Chen et al., 2009). However, rather than ET forming enzymes (EFE), *Fg* was thought to use pathways incorporating 1-aminocyclopropane carboxylic acids (ACC) as precursors for ET biosynthesis (Svoboda et al., 2019). Although an enzymatic function for two of the five ACC enzymes encoded by the *Fg* genome could be confirmed, fungal mutants for these genes showed no defect in pathogenicity on wheat (Svoboda et al., 2019). We looked at the expression of all these five genes, including the three annotated *ACC synthase* genes, *FG05_05184* (*ACS1*), *FG05_07606* (*ACS2*), *FG05_13587* (*ACS3*), and two *ACC deaminase* (*ACD*) genes, *FG05_02678* and *FG05_12669*, but found no differential expression during *Bd* root infections (Table S1), suggesting that pathogen produced ET may not be involved in root infection.

Biosynthesis of fungal cytokinins, which can be mediated by either one or both of the fungal transfer RNA-isopentenyl transferases (tRNA-IPT) and the Lonely Guy (LOG) enzyme, is associated with host immunity and nutrient modulation and maintenance of hemi-biotrophic lifestyles during infection (Spallek et al., 2018). Unlike many other *Fusarium* species, the *Fg* genome contains only one tRNA-IPT gene homolog (*FG05_09015*) (Sørensen et al., 2018). This gene was not differentially regulated (Table S1) and only moderately expressed (FPKM < 10) during both root infections and *in vitro* growth on MM.

Exogenous ABA has no effects on disease development, *Fg* toxin production or defense hormone levels in *Fg*-challenged wheat heads, but can promote fungal hydrolase and cytoskeletal reorganization genes induced early during infection and increase wheat's susceptibility to FHB (Buhrow et al., 2016). The elucidation of fungal genes responsible for ABA production in the necrotrophic pathogen *Botrytis cinerea* and a few others has led to the hypothesis that a conserved ABA biosynthesis pathway exists in fungi (Lievens et al., 2017). In *B. cinerea*, such pathway involves four clustered genes *BcABA1-4* and a sesquiterpene cyclase gene *BcSTC5* (Izquierdo-Bueno et al., 2018). Fungal ABA was shown to act as a

693 virulence factor in *M. oryzae*, which also harbors a direct ABA biosynthesis pathway but
694 lacks a BsABA3 ortholog (Spence et al., 2015). Similar to *M. oryzae*, we could identify
695 homologs of only BcABA1, 2 and 4 by BLASTp in *Fg*. In the current root transcriptome, none
696 of these genes was differentially regulated (Table S1). Overall, while fungal GAs and IAAs
697 might be associated with *Fg* root infections, it is unlikely that ETs, CKs and ABAs are
698 involved in *Bd* root infection by *Fg*.

699 **Conclusions**

700 The results presented here provide a detailed overview of root infection strategies employed
701 by *Fg*, an important cereal fungal pathogen. The transcriptional regulation of pathogen
702 metabolic pathways, virulence factors and signalling events during root infection show both
703 unique and common features to those employed by *Fg* when infecting above-ground tissues.
704 The mycotoxin DON, although not required for fungal virulence, produced during root
705 infection appears to broadly affect various fungal processes and interplay with host
706 responses. Expressions of several fungal stress and defence genes might help the pathogen
707 to effectively deal with plant defence responses. In line with this, fungal JA, IAA and, in
708 particular SA, seem to be used to interfere with root defenses. The findings presented in this
709 paper will be useful for dissecting the mechanism of *Fg* belowground lifestyle and the
710 development of novel plant protection strategies.

711 **Acknowledgements**

712 We thank Di Xiao and Dr. Jonathan Powell for technical assistance. Yi Ding was the
713 recipient of a post-doctoral fellowship from the Commonwealth Scientific and Industrial
714 Research Organization Research Office.

715 **Conflict of interest**

716 All authors declared no conflict of interest.

717 **References**

718 Abou Ammar, G., Tryono, R., Döll, K., Karlovsky, P., Deising, H.B., Wirsel, S.G.R., 2013.
719 Identification of ABC Transporter Genes of Fusarium graminearum with Roles in Azole
720 Tolerance and/or Virulence. PLoS One 8, e79042.
721 https://doi.org/10.1371/journal.pone.0079042

722 Audenaert, K., Vanheule, A., Höfte, M., Haesaert, G., 2013. Deoxynivalenol: A major player
723 in the multifaceted response of Fusarium to its environment. Toxins (Basel). 6, 1–19.
724 https://doi.org/10.3390/toxins6010001

725 Bhandari, D.R., Wang, Q., Li, B., Friedt, W., Römpp, A., Spengler, B., Gottwald, S., 2018.
726 Histology-guided high-resolution AP-SMALDI mass spectrometry imaging of wheat-
727 Fusarium graminearum interaction at the root-shoot junction. Plant Methods 14, 1–13.
728 https://doi.org/10.1186/s13007-018-0368-6

729 Bhuiyan, N.H., Selvaraj, G., Wei, Y., King, J., 2009. Role of lignification in plant defense.
730 Plant Signal. Behav. 4, 158–159. https://doi.org/10.4161/psb.4.2.7688

731 Boedi, S., Berger, H., Sieber, C., Münsterkötter, M., Maloku, I., Warth, B., Sulyok, M.,
732 Lemmens, M., Schuhmacher, R., Güldener, U., Strauss, J., 2016. Comparison of
733 Fusarium graminearum transcriptomes on living or dead wheat differentiates substrate-
734 responsive and defense-responsive genes. Front. Microbiol. 7, 1–24.
735 https://doi.org/10.3389/fmicb.2016.01113

736 Boenisch, M.J., Schäfer, W., 2011. Fusarium graminearum forms mycotoxin producing
737 infection structures on wheat. BMC Plant Biol. 11, 110. https://doi.org/10.1186/1471-
738 2229-11-110

739 Bönnighausen, J., Schauer, N., Schäfer, W., Bormann, J., 2019. Metabolic profiling of wheat
740 rachis node infection by Fusarium graminearum – decoding deoxynivalenol-dependent
741 susceptibility. New Phytol. 221, 459–469. https://doi.org/10.1111/nph.15377

742 Brauer, E.K., Balcerzak, M., Rocheleau, H., Leung, W., Schernthaner, J., Subramaniam, R.,

743 Ouellet, T., 2020. Genome Editing of a Deoxynivalenol-Induced Transcription Factor
744 Confers Resistance to Fusarium graminearum in Wheat. Mol. Plant-Microbe Interact.
745 33, 553–560. https://doi.org/10.1094/MPMI-11-19-0332-R

746 Brodhun, F., Cristobal-Sarramian, A., Zabel, S., Newie, J., Hamberg, M., Feussner, I., 2013.
747 An Iron 13S-Lipoxygenase with an α-Linolenic Acid Specific Hydroperoxidase Activity
748 from Fusarium oxysporum. PLoS One 8. https://doi.org/10.1371/journal.pone.0064919

749 Brown, N.A., Antoniw, J., Hammond-Kosack, K.E., 2012. The predicted secretome of the
750 plant pathogenic fungus Fusarium graminearum: A refined comparative analysis. PLoS
751 One 7. https://doi.org/10.1371/journal.pone.0033731

752 Brown, N.A., Evans, J., Mead, A., Hammond-Kosack, K.E., 2017. A spatial temporal analysis
753 of the Fusarium graminearum transcriptome during symptomless and symptomatic
754 wheat infection. Mol. Plant Pathol. 18, 1295–1312. https://doi.org/10.1111/mpp.12564

755 Buhrow, L.M., Cram, D., Tulpan, D., Foroud, N.A., Loewen, M.C., 2016. Exogenous abscisic
756 acid and gibberellic acid elicit opposing effects on Fusarium graminearum infection in
757 wheat. Phytopathology 106, 986–996. https://doi.org/10.1094/PHYTO-01-16-0033-R

758 Caarls, L., Elberse, J., Awwanah, M., Ludwig, N.R., De Vries, M., Zeilmaker, T., Van Wees,
759 S.C.M., Schuurink, R.C., Van den Ackerveken, G., 2017. Arabidopsis JASMONATE-
760 INDUCED OXYGENASES down-regulate plant immunity by hydroxylation and
761 inactivation of the hormone jasmonic acid. Proc. Natl. Acad. Sci. U. S. A. 114, 6388–
762 6393. https://doi.org/10.1073/pnas.1701101114

763 Chanclud, E., Morel, J.-B., 2016. Plant hormones: a fungal point of view. Mol. Plant Pathol.
764 17, 1289–1297. https://doi.org/10.1111/mpp.12393

765 Chen, F., Zhang, J., Song, X., Yang, J., Li, H., Tang, H., Liao, Y.C., 2011. Combined
766 metabonomic and quantitative real-time PCR analyses reveal systems metabolic
767 changes of Fusarium graminearum induced by Tri5 gene deletion. J. Proteome Res. 10,

768 2273–2285. https://doi.org/10.1021/pr101095t

769 Chen, X., Steed, A., Travella, S., Keller, B., Nicholson, P., 2009. Fusarium graminearum
770 exploits ethylene signalling to colonize dicotyledonous and monocotyledonous plants.
771 New Phytol. 182, 975–983. https://doi.org/10.1111/j.1469-8137.2009.02821.x

772 Chen, Y., Kistler, H.C., Ma, Z., 2019. Fusarium graminearum Trichothecene Mycotoxins:
773 Biosynthesis, Regulation, and Management . Annu. Rev. Phytopathol. 57, 1–25.
774 https://doi.org/10.1146/annurev-phyto-082718-100318

775 Coleman, J.J., Mylonakis, E., 2009. Efflux in fungi: La pièce de résistance. PLoS Pathog. 5.
776 https://doi.org/10.1371/journal.ppat.1000486

777 Cuzick, A., Urban, M., Hammond-Kosack, K., 2008. Fusarium graminearum gene deletion
778 mutants map1 and tri5 reveal similarities and differences in the pathogenicity
779 requirements to cause disease on Arabidopsis and wheat floral tissue. New Phytol. 177,
780 990–1000. https://doi.org/10.1111/j.1469-8137.2007.02333.x

781 De Jonge, R., Esse, H.P. Van, Kombrink, A., Shinya, T., Desaki, Y., Bours, R., Krol, S. Van
782 Der, Shibuya, N., Joosten, M.H. a J., Thomma, B.P.H.J., 2010. Immunity in Plants.
783 Science (80-.). 329, 953–955. https://doi.org/10.1126/science.1190859

784 Desmond, O.J., Manners, J.M., Stephens, A.E., Maclean, D.J., Schenk, P.M., Gardiner,
785 D.M., Munn, A.L., Kazan, K., 2008. The Fusarium mycotoxin deoxynivalenol elicits
786 hydrogen peroxide production, programmed cell death and defence responses in wheat.
787 Mol. Plant Pathol. 9, 435–445. https://doi.org/10.1111/j.1364-3703.2008.00475.x

788 Diamond, M., Reape, T.J., Rocha, O., Doyle, S.M., Kacprzyk, J., Doohan, F.M., McCabe,
789 P.F., 2013. The Fusarium Mycotoxin Deoxynivalenol Can Inhibit Plant Apoptosis-Like
790 Programmed Cell Death. PLoS One 8. https://doi.org/10.1371/journal.pone.0069542

791 Ding, L., Xu, H., Yi, H., Yang, L., Kong, Z., Zhang, L., Xue, S., Jia, H., Ma, Z., 2011.
792 Resistance to hemi-biotrophic f. graminearum infection is associated with coordinated

and ordered expression of diverse defense signaling pathways. PLoS One 6. https://doi.org/10.1371/journal.pone.0019008

Ding, Y., Gardiner, D.M., Xiao, D., Kazan, K., 2020. Regulators of nitric oxide signaling triggered by host perception in a plant pathogen. Proc. Natl. Acad. Sci. 201918977. https://doi.org/10.1073/pnas.1918977117

Divon, H.H., Fluhr, R., 2007. Nutrition acquisition strategies during fungal infection of plants. FEMS Microbiol. Lett. 266, 65–74. https://doi.org/10.1111/j.1574-6968.2006.00504.x

Dutartre, L., Hilliou, F., Feyereisen, R., 2012. Phylogenomics of the benzoxazinoid biosynthetic pathway of Poaceae: Gene duplications and origin of the B× cluster. BMC Evol. Biol. 12. https://doi.org/10.1186/1471-2148-12-64

Fischer, G.J., Keller, N.P., 2016. Production of cross-kingdom oxylipins by pathogenic fungi: An update on their role in development and pathogenicity. J. Microbiol. 54, 254–264. https://doi.org/10.1007/s12275-016-5620-z

Fitzgerald, T.L., Powell, J.J., Schneebeli, K., Hsia, M.M., Gardiner, D.M., Bragg, J.N., McIntyre, C.L., Manners, J.M., Ayliffe, M., Watt, M., Vogel, J.P., Henry, R.J., Kazan, K., 2015. Brachypodium as an emerging model for cereal–pathogen interactions. Ann. Bot. 115, 717–731. https://doi.org/10.1093/aob/mcv010

Foroud, N.A., Pordel, R., Goyal, R.K., Ryabova, D., Eranthodi, A., Chatterton, S., Kovalchuk, I., 2019. Chemical Activation of the Ethylene Signaling Pathway Promotes Fusarium graminearum Resistance in Detached Wheat Heads. Phytopathology 109, 796–803. https://doi.org/10.1094/PHYTO-08-18-0286-R

Gardiner, D.M., Benfield, A.H., Stiller, J., Stephen, S., Aitken, K., Liu, C., Kazan, K., 2018. A high-resolution genetic map of the cereal crown rot pathogen Fusarium pseudograminearum provides a near-complete genome assembly. Mol. Plant Pathol. 19, 217–226. https://doi.org/10.1111/mpp.12519

818 Gardiner, D.M., Kazan, K., Manners, J.M., 2009. Nutrient profiling reveals potent inducers of
819 trichothecene biosynthesis in Fusarium graminearum. Fungal Genet. Biol. 46, 604–613.
820 https://doi.org/10.1016/j.fgb.2009.04.004

821 Gardiner, D.M., Kazan, K., Praud, S., Torney, F.J., Rusu, A., Manners, J.M., 2010. Early
822 activation of wheat polyamine biosynthesis during Fusarium head blight implicates
823 putrescine as an inducer of trichothecene mycotoxin production. BMC Plant Biol. 10,
824 289. https://doi.org/10.1186/1471-2229-10-289

825 Gardiner, D.M., Stephens, A.E., Munn, A.L., Manners, J.M., 2013. An ABC pleiotropic drug
826 resistance transporter of fusarium graminearum with a role in crown and root diseases
827 of wheat. FEMS Microbiol. Lett. 348, 36–45. https://doi.org/10.1111/1574-6968.12240

828 Gardiner, D.M., Stiller, J., Kazan, K., 2014. Genome sequence of Fusarium graminearum
829 isolate CS3005. Genome Announc. 2, e00227-14-e00227-14.
830 https://doi.org/10.1128/genomeA.00227-14

831 Gatti, M., Cambon, F., Tassy, C., Macadre, C., Guerard, F., Langin, T., Dufresne, M., 2019.
832 The Brachypodium distachyon UGT Bradi5gUGT03300 confers type II fusarium head
833 blight resistance in wheat. Plant Pathol. 68, 334–343. https://doi.org/10.1111/ppa.12941

834 Gatti, M., Cambon, F., Tassy, C., Macadre, C., Guerard, F., Langin, T., Dufresne, M., 2018.
835 The *Brachypodium distachyon* UGT Bradi5gUGT03300 confers type II Fusarium Head
836 Blight resistance in wheat. Plant Pathol. https://doi.org/10.1111/ppa.12941

837 Glazebrook, J., 2005. Contrasting Mechanisms of Defense Against Biotrophic and
838 Necrotrophic Pathogens. Annu. Rev. Phytopathol. 43, 205–227.
839 https://doi.org/10.1146/annurev.phyto.43.040204.135923

840 Götz, S., García-Gómez, J.M., Terol, J., Williams, T.D., Nagaraj, S.H., Nueda, M.J., Robles,
841 M., Talón, M., Dopazo, J., Conesa, A., 2008. High-throughput functional annotation and
842 data mining with the Blast2GO suite. Nucleic Acids Res.

https://doi.org/10.1093/nar/gkn176

Güldener, U., Mannhaupt, G., Münsterkötter, M., Haase, D., Oesterheld, M., Stümpflen, V., Mewes, H.-W., Adam, G., 2006. FGDB: a comprehensive fungal genome resource on the plant pathogen Fusarium graminearum. Nucleic Acids Res. 34, D456-8. https://doi.org/10.1093/nar/gkj026

Guo, L., Breakspear, A., Zhao, G., Gao, L., Kistler, H.C., Xu, J.R., Ma, L.J., 2016. Conservation and divergence of the cyclic adenosine monophosphate-protein kinase A (cAMP-PKA) pathway in two plant-pathogenic fungi: Fusarium graminearum and F.verticillioides. Mol. Plant Pathol. 17, 196–209. https://doi.org/10.1111/mpp.12272

Hao, G., Naumann, T.A., Vaughan, M.M., McCormick, S., Usgaard, T., Kelly, A., Ward, T.J., 2019. Characterization of a Fusarium graminearum salicylate hydroxylase. Front. Microbiol. 10, 1–11. https://doi.org/10.3389/fmicb.2018.03219

Harris, L.J., Balcerzak, M., Johnston, A., Schneiderman, D., Ouellet, T., 2016. Host-preferential Fusarium graminearum gene expression during infection of wheat, barley, and maize. Fungal Biol. 120, 111–123. https://doi.org/10.1016/j.funbio.2015.10.010

Hart, T., Komori, H.K., LaMere, S., Podshivalova, K., Salomon, D.R., 2013. Finding the active genes in deep RNA-seq gene expression studies. BMC Genomics 14. https://doi.org/10.1186/1471-2164-14-778

Hellin, P., King, R., Urban, M., Hammond-Kosack, K.E., Legrève, A., 2018. The adaptation of Fusarium culmorum to DMI fungicides is mediated by major transcriptome modifications in response to azole fungicide, including the overexpression of a PDR transporter (FcABC1). Front. Microbiol. 9, 1–15. https://doi.org/10.3389/fmicb.2018.01385

Henkes, G.J., Jousset, A., Bonkowski, M., Thorpe, M.R., Scheu, S., Lanoue, A., Schurr, U., Röse, U.S.R., 2011. Pseudomonas fluorescens CHA0 maintains carbon delivery to

868 Fusarium graminearum-infected roots and prevents reduction in biomass of barley
869 shoots through systemic interactions. J. Exp. Bot. 62, 4337–4344.
870 https://doi.org/10.1093/jxb/err149

871 Hohn, T.M., Beremand, P.D., 1989. Isolation and nucleotide sequence of a sesquiterpene
872 cyclase gene from the trichothecene-producing fungus Fusarium sporotrichioides. Gene
873 79, 131–138. https://doi.org/10.1016/0378-1119(89)90098-X

874 Izquierdo-Bueno, I., González-Rodríguez, V.E., Simon, A., Dalmais, B., Pradier, J.M., Le
875 Pêcheur, P., Mercier, A., Walker, A.S., Garrido, C., Collado, I.G., Viaud, M., 2018.
876 Biosynthesis of abscisic acid in fungi: identification of a sesquiterpene cyclase as the
877 key enzyme in Botrytis cinerea. Environ. Microbiol. 20, 2469–2482.
878 https://doi.org/10.1111/1462-2920.14258

879 Jansen, C., von Wettstein, D., Schäfer, W., Kogel, K.-H., Felk, A., Maier, F.J., 2005. Infection
880 patterns in barley and wheat spikes inoculated with wild-type and trichodiene synthase
881 gene disrupted Fusarium graminearum. Proc. Natl. Acad. Sci. U. S. A. 102, 16892–7.
882 https://doi.org/10.1073/pnas.0508467102

883 Jashni, M.K., Dols, I.H.M., Iida, Y., Boeren, S., Beenen, H.G., Mehrabi, R., 2015. Synergistic
884 Action of a Metalloprotease and a Serine Protease from Fusarium oxysporum f. sp.
885 lycopersici Cleaves Chitin-Binding Tomato Chitinases, Reduces Their Antifungal
886 Activity, and Enhances Fungal Virulence 28, 996–1008.

887 Kazan, K., Gardiner, D.M., 2018a. Transcriptomics of cereal–Fusarium graminearum
888 interactions: what we have learned so far. Mol. Plant Pathol. 19, 764–778.
889 https://doi.org/10.1111/mpp.12561

890 Kazan, K., Gardiner, D.M., 2018b. Fusarium crown rot caused by Fusarium
891 pseudograminearum in cereal crops: recent progress and future prospects. Mol. Plant
892 Pathol. 19, 1547–1562. https://doi.org/10.1111/mpp.12639

893 Kazan, K., Lyons, R., 2014. Intervention of Phytohormone Pathways by Pathogen Effectors.
894 Plant Cell 26, 2285–2309. https://doi.org/10.1105/tpc.114.125419

895 Kazan, K., Manners, J.M., 2009. Linking development to defense: auxin in plant-pathogen
896 interactions. Trends Plant Sci. 14, 373–382.
897 https://doi.org/10.1016/j.tplants.2009.04.005

898 Khan, N.U., Liu, M., Yang, X., Qiu, D., 2016. Fungal elicitor MoHrip2 induces disease
899 resistance in rice leaves, triggering stress-related pathways. PLoS One 11, 1–14.
900 https://doi.org/10.1371/journal.pone.0158112

901 Kim, H.-K., Jo, S.-M., Kim, G.-Y., Kim, D.-W., Kim, Y.-K., Yun, S.-H., 2015. A Large-Scale
902 Functional Analysis of Putative Target Genes of Mating-Type Loci Provides Insight into
903 the Regulation of Sexual Development of the Cereal Pathogen Fusarium graminearum.
904 PLoS Genet. 11, e1005486. https://doi.org/10.1371/journal.pgen.1005486

905 Lanoue, A., Burlat, V., Henkes, G.J., Koch, I., Schurr, U., Röse, U.S.R., 2010. De novo
906 biosynthesis of defense root exudates in response to Fusarium attack in barley. New
907 Phytol. 185, 577–588. https://doi.org/10.1111/j.1469-8137.2009.03066.x

908 Larochelle, M., Drouin, S., Robert, F., Turcotte, B., 2006. Oxidative Stress-Activated Zinc
909 Cluster Protein Stb5 Has Dual Activator/Repressor Functions Required for Pentose
910 Phosphate Pathway Regulation and NADPH Production. Mol. Cell. Biol. 26, 6690–6701.
911 https://doi.org/10.1128/mcb.02450-05

912 Lee, J., Son, H., Lee, S., Park, A.R., Lee, Y.W., 2010. Development of a conditional gene
913 expression system using a zearalenone-inducible promoter for the ascomycete fungus
914 gibberella zeae. Appl. Environ. Microbiol. 76, 3089–3096.
915 https://doi.org/10.1128/AEM.02999-09

916 Li, G., Yen, Y., 2008. Jasmonate and ethylene signaling pathway may mediate Fusarium
917 head blight resistance in wheat. Crop Sci. 48, 1888–1896.

https://doi.org/10.2135/cropsci2008.02.0097

Liang, Y., Cui, S., Tang, X., Zhang, Y., Qiu, D., Zeng, H., Guo, L., Yuan, J., Yang, X., 2018. An Asparagine-Rich Protein Nbnrp1 Modulate Verticillium dahliae Protein PevD1-Induced Cell Death and Disease Resistance in Nicotiana benthamiana. Front. Plant Sci. 9, 303. https://doi.org/10.3389/fpls.2018.00303

Lievens, L., Pollier, J., Goossens, A., Beyaert, R., Staal, J., 2017. Abscisic acid as pathogen effector and immune regulator. Front. Plant Sci. 8, 1–15. https://doi.org/10.3389/fpls.2017.00587

Lindo, L., McCormick, S.P., Cardoza, R.E., Brown, D.W., Kim, H.S., Alexander, N.J., Proctor, R.H., Gutiérrez, S., 2018. Effect of deletion of a trichothecene toxin regulatory gene on the secondary metabolism transcriptome of the saprotrophic fungus Trichoderma arundinaceum. Fungal Genet. Biol. 119, 29–46. https://doi.org/10.1016/j.fgb.2018.08.002

Lindo, L., McCormick, S.P., Cardoza, R.E., Kim, H.S., Brown, D.W., Alexander, N.J., Proctor, R.H., Gutiérrez, S., 2019. Role of Trichoderma arundinaceum tri10 in regulation of terpene biosynthetic genes and in control of metabolic flux. Fungal Genet. Biol. 122, 31–46. https://doi.org/10.1016/j.fgb.2018.11.001

Liu, T., Song, T., Zhang, X., Yuan, H., Su, L., Li, W., Xu, J., Liu, S., Chen, L., Chen, T., Zhang, M., Gu, L., Zhang, B., Dou, D., 2014. Unconventionally secreted effectors of two filamentous pathogens target plant salicylate biosynthesis. Nat. Commun. 5. https://doi.org/10.1038/ncomms5686

Lo Presti, L., Lanver, D., Schweizer, G., Tanaka, S., Liang, L., Tollot, M., Zuccaro, A., Reissmann, S., Kahmann, R., 2015. Fungal Effectors and Plant Susceptibility. Annu. Rev. Plant Biol. 66, 513–545. https://doi.org/10.1146/annurev-arplant-043014-114623

Lu, S., Edwards, M.C., 2016. Genome-Wide Analysis of Small Secreted Cysteine-Rich

943 Proteins Identifies Candidate Effector Proteins Potentially Involved in Fusarium
944 graminearum-Wheat Interactions. Phytopathology 106, 166–176.
945 https://doi.org/10.1094/PHYTO-09-15-0215-R

946 Luo, K., Rocheleau, H., Qi, P.F., Zheng, Y.L., Zhao, H.Y., Ouellet, T., 2016. Indole-3-acetic
947 acid in Fusarium graminearum: Identification of biosynthetic pathways and
948 characterization of physiological effects. Fungal Biol. 120, 1135–1145.
949 https://doi.org/10.1016/j.funbio.2016.06.002

950 Lyons, R., Stiller, J., Powell, J., Rusu, A., Manners, J.M., Kazan, K., 2015. Fusarium
951 oxysporum triggers tissue-specific transcriptional reprogramming in Arabidopsis
952 thaliana. PLoS One 10, 1–23. https://doi.org/10.1371/journal.pone.0121902

953 Lysøe, E., Seong, K., Kistler, H.C., 2011. The Transcriptome of Fusarium graminearum
954 During the Infection of Wheat. Mol. Plant-Microbe Interact. 24, 995–1000.
955 https://doi.org/10.1094/MPMI-02-11-0038

956 Ma, L.-J., Geiser, D.M., Proctor, R.H., Rooney, A.P., O'Donnell, K., Trail, F., Gardiner, D.M.,
957 Manners, J.M., Kazan, K., 2013. *Fusarium* Pathogenomics. Annu. Rev. Microbiol. 67,
958 399–416. https://doi.org/10.1146/annurev-micro-092412-155650

959 Makandar, R., Nalam, V., Chaturvedi, R., Jeannotte, R., Sparks, A.A., Shah, J., 2010.
960 Involvement of Salicylate and Jasmonate Signaling Pathways in Arabidopsis Interaction
961 with Fusarium graminearum. Mol. Plant-Microbe Interact. 23, 861–870.
962 https://doi.org/10.1094/MPMI-23-7-0861

963 Malz, S., Grell, M.N., Thrane, C., Maier, F.J., Rosager, P., Felk, A., Albertsen, K.S., Salomon,
964 S., Bohn, L., Schäfer, W., Giese, H., 2005. Identification of a gene cluster responsible
965 for the biosynthesis of aurofusarin in the Fusarium graminearum species complex.
966 Fungal Genet. Biol. 42, 420–433. https://doi.org/10.1016/j.fgb.2005.01.010

967 Mano, Y., Nemoto, K., 2012. The pathway of auxin biosynthesis in plants. J. Exp. Bot. 63,

2853–2872. https://doi.org/10.1093/jxb/ers091

Marcel, S., Sawers, R., Oakeley, E., Angliker, H., Paszkowski, U., 2010. Tissue-Adapted Invasion Strategies of the Rice Blast Fungus *Magnaporthe oryzae*. Plant Cell 22, 3177–3187. https://doi.org/10.1105/tpc.110.078048

Marshall, R., Kombrink, A., Motteram, J., Loza-Reyes, E., Lucas, J., Hammond-Kosack, K.E., Thomma, B.P.H.J., Rudd, J.J., 2011. Analysis of Two in Planta Expressed LysM Effector Homologs from the Fungus Mycosphaerella graminicola Reveals Novel Functional Properties and Varying Contributions to Virulence on Wheat. Plant Physiol. 156, 756–769. https://doi.org/10.1104/pp.111.176347

Masuda, D., Ishida, M., Yamaguchi, K., Yamaguchi, I., Kimura, M., Nishiuchi, T., 2007. Phytotoxic effects of trichothecenes on the growth and morphology of Arabidopsis thaliana. J. Exp. Bot. 58, 1617–1626. https://doi.org/10.1093/jxb/erl298

Mazaheri-Naeini, M., Sabbagh, S.K., Martinez, Y., Séjalon-Delmas, N., Roux, C., 2015. Assessment of Ustilago maydis as a fungal model for root infection studies. Fungal Biol. 119, 145–153. https://doi.org/10.1016/j.funbio.2014.12.002

Mentlak, T.A., Kombrink, A., Shinya, T., Ryder, L.S., Otomo, I., Saitoh, H., Terauchi, R., Nishizawa, Y., Shibuya, N., Thomma, B.P.H.J., Talbot, N.J., 2012. Effector-Mediated Suppression of Chitin-Triggered Immunity by Magnaporthe oryzae Is Necessary for Rice Blast Disease. Plant Cell 24, 322–335. https://doi.org/10.1105/tpc.111.092957

Moscetti, I., Faoro, F., Moro, S., Sabbadin, D., Sella, L., Favaron, F., D'Ovidio, R., 2015. The xylanase inhibitor TAXI-III counteracts the necrotic activity of a Fusarium graminearum xylanase in vitro and in durum wheat transgenic plants. Mol. Plant Pathol. 16, 583–592. https://doi.org/10.1111/mpp.12215

Mudge, A.M., Dill-Macky, R., Dong, Y., Gardiner, D.M., White, R.G., Manners, J.M., 2006. A role for the mycotoxin deoxynivalenol in stem colonisation during crown rot disease of

993 wheat caused by Fusarium graminearum and Fusarium pseudograminearum. Physiol.
994 Mol. Plant Pathol. 69, 73–85. https://doi.org/10.1016/j.pmpp.2007.01.003

995 Navarro, L., Bari, R., Achard, P., Lisón, P., Nemri, A., Harberd, N.P., Jones, J.D.G., 2008.
996 DELLAs Control Plant Immune Responses by Modulating the Balance of Jasmonic Acid
997 and Salicylic Acid Signaling. Curr. Biol. 18, 650–655.
998 https://doi.org/10.1016/j.cub.2008.03.060

999 Oide, S., Berthiller, F., Wiesenberger, G., Adam, G., Turgeon, B.G., 2014. Individual and
1000 combined roles of malonichrome, ferricrocin, and TAFC siderophores in Fusarium
1001 graminearum pathogenic and sexual development. Front. Microbiol. 5, 1–15.
1002 https://doi.org/10.3389/fmicb.2014.00759

1003 Pan, Y., Liu, Z., Rocheleau, H., Fauteux, F., Wang, Y., McCartney, C., Ouellet, T., 2018.
1004 Transcriptome dynamics associated with resistance and susceptibility against fusarium
1005 head blight in four wheat genotypes. BMC Genomics 19, 1–26.
1006 https://doi.org/10.1186/s12864-018-5012-3

1007 Pasquet, J.-C., Changenet, V., Macadré, C., Boex-Fontvieille, E., Soulhat, C., Bouchabké-
1008 Coussa, O., Dalmais, M., Atanasova-Pénichon, V., Bendahmane, A., Saindrenan, P.,
1009 Dufresne, M., 2016. A Brachypodium UDP-glycosytransferase confers root tolerance to
1010 deoxynivalenol and resistance to Fusarium infection. Plant Physiol. 172, 559–574.
1011 https://doi.org/10.1104/pp.16.00371

1012 Pasquet, J.-C.C., Chaouch, S., Macadré, C., Balzergue, S., Huguet, S., Martin-Magniette,
1013 M.-L.L., Bellvert, F., Deguercy, X., Thareau, V., Heintz, D., Saindrenan, P., Dufresne,
1014 M., 2014. Differential gene expression and metabolomic analyses of Brachypodium
1015 distachyon infected by deoxynivalenol producing and non-producing strains of
1016 Fusarium graminearum. BMC Genomics 15, 1–17. https://doi.org/10.1186/1471-2164-
1017 15-629

1018 Patkar, R.N., Naqvi, N.I., 2017. Fungal manipulation of hormone-regulated plant defense.

1019 PLoS Pathog. 13, 10–14. https://doi.org/10.1371/journal.ppat.1006334

1020 Pieterse, C.M.J., Leon-Reyes, A., Van Der Ent, S., Van Wees, S.C.M., 2009. Networking by
1021 small-molecule hormones in plant immunity. Nat. Chem. Biol. 5, 308–316.
1022 https://doi.org/10.1038/nchembio.164

1023 Pieterse, C.M.J., Van der Does, D., Zamioudis, C., Leon-Reyes, A., Van Wees, S.C.M.,
1024 2012. Hormonal Modulation of Plant Immunity. Annu. Rev. Cell Dev. Biol. 28, 489–521.
1025 https://doi.org/10.1146/annurev-cellbio-092910-154055

1026 Powell, J.J., Carere, J., Sablok, G., Fitzgerald, T.L., Stiller, J., Colgrave, M.L., Gardiner, D.M.,
1027 Manners, J.M., Vogel, J.P., Henry, R.J., Kazan, K., 2017. Transcriptome analysis of
1028 Brachypodium during fungal pathogen infection reveals both shared and distinct
1029 defense responses with wheat. Sci. Rep. 7, 1–14. https://doi.org/10.1038/s41598-017-
1030 17454-3

1031 Proctor, R.H., Hohn, T.M., McCormick, S.P., 1995. Reduced virulence of Gibberella zeae
1032 caused by disruption of a trichothecene toxin biosynthetic gene. Mol. Plant. Microbe.
1033 Interact. 8, 593–601.

1034 Puri, K.D., Yan, C., Leng, Y., Zhong, S., 2016. RNA-seq revealed differences in
1035 transcriptomes between 3ADON and 15ADON populations of Fusarium graminearum in
1036 vitro and in planta. PLoS One 11, 1–30. https://doi.org/10.1371/journal.pone.0163803

1037 Qi, P.-F., Zhang, Y.-Z., Liu, C.-H., Chen, Q., Guo, Z.-R., Wang, Y., Xu, B.-J., Jiang, Y.-F.,
1038 Zheng, T., Gong, X., Luo, C.-H., Wu, W., Kong, L., Deng, M., Ma, J., Lan, X.-J., Jiang,
1039 Q.-T., Wei, Y.-M., Wang, J.-R., Zheng, Y.-L., 2019. Functional Analysis of FgNahG
1040 Clarifies the Contribution of Salicylic Acid to Wheat (Triticum aestivum) Resistance
1041 against Fusarium Head Blight. Toxins (Basel). 11, 59.
1042 https://doi.org/10.3390/toxins11020059

1043 Qi, P.F., Balcerzak, M., Rocheleau, H., Leung, W., Wei, Y.M., Zheng, Y.L., Ouellet, T., 2016.

Jasmonic acid and abscisic acid play important roles in host-pathogen interaction between Fusarium graminearum and wheat during the early stages of fusarium head blight. Physiol. Mol. Plant Pathol. 93, 39–48. https://doi.org/10.1016/j.pmpp.2015.12.004

Quarantin, A., Glasenapp, A., Schäfer, W., Favaron, F., Sella, L., 2016. Involvement of the Fusarium graminearum cerato-platanin proteins in fungal growth and plant infection. Plant Physiol. Biochem. 109, 220–229. https://doi.org/10.1016/j.plaphy.2016.10.001

Rabe, F., Ajami-Rashidi, Z., Doehlemann, G., Kahmann, R., Djamei, A., 2013. Degradation of the plant defence hormone salicylic acid by the biotrophic fungus Ustilago maydis. Mol. Microbiol. 89, 179–188. https://doi.org/10.1111/mmi.12269

Reineke, G., Heinze, B., Schirawski, J., Buettner, H., Kahmann, R., Basse, C.W., 2008. Indole-3-acetic acid (IAA) biosynthesis in the smut fungus Ustilago maydis and its relevance for increased IAA levels in infected tissue and host tumour formation. Mol. Plant Pathol. 9, 339–355. https://doi.org/10.1111/j.1364-3703.2008.00470.x

Rocheleau, H., Al-harthi, R., Ouellet, T., 2019. Degradation of salicylic acid by Fusarium graminearum. Fungal Biol. 123, 77–86. https://doi.org/10.1016/j.funbio.2018.11.002

Scherm, B., Balmas, V., Spanu, F., Pani, G., Delogu, G., Pasquali, M., Migheli, Q., 2013a. Fusarium culmorum: Causal agent of foot and root rot and head blight on wheat. Mol. Plant Pathol. 14, 323–341. https://doi.org/10.1111/mpp.12011

Scherm, B., Balmas, V., Spanu, F., Pani, G., Delogu, G., Pasquali, M., Migheli, Q., Johansson, P.M., Johnsson, L., Gerhardson, B., Hope, R., Aldred, D., Magan, N., Cuomo, C.A., Güldener, U., Xu, J., Trail, F., Turgeon, B.G., Pietro, A. Di, Walton, J.D., Ma, L., Baker, S.E., Rep, M., Adam, G., Antoniw, J., Baldwin, T., Calvo, S., Chang, Y., Harris, L.J., Hilburn, K., Kennell, J.C., Kroken, S., Magnuson, J.K., Muehlbauer, G., Münsterkötter, M., Nelson, D., Donnell, K.O., Ouellet, T., 2013b. The Fusarium graminearum Genome. Mol. Plant Pathol. 14, 295–300.

https://doi.org/10.1126/science.1143708

Schuler, D., Wahl, R., Wippel, K., Vranes, M., Münsterkötter, M., Sauer, N., Kämper, J., 2015. Hxt1, a monosaccharide transporter and sensor required for virulence of the maize pathogen Ustilago maydis. New Phytol. 206, 1086–1100. https://doi.org/10.1111/nph.13314

Serino, L., Reimmann, C., Baur, H., Beyeler, M., Visca, P., Haas, D., 1995. Structural genes for salicylate biosynthesis from chorismate in Pseudomonas aeruginosa. Mgg Mol. Gen. Genet. 249, 217–228. https://doi.org/10.1007/BF00290369

Sesma, A., Osbourn, A.E., 2004. The rice leaf blast pathogen undergoes developmental processes typical of root-infecting fungi. Nature 431, 582–586. https://doi.org/10.1038/nature02880

Sieber, C.M.K., Lee, W., Wong, P., Münsterkötter, M., Mewes, H.-W., Schmeitzl, C., Varga, E., Berthiller, F., Adam, G., Güldener, U., 2014. The Fusarium graminearum genome reveals more secondary metabolite gene clusters and hints of horizontal gene transfer. PLoS One 9, e110311. https://doi.org/10.1371/journal.pone.0110311

Smirnova, E., Marquis, V., Poirier, L., Aubert, Y., Zumsteg, J., Ménard, R., Miesch, L., Heitz, T., 2017. Jasmonic Acid Oxidase 2 Hydroxylates Jasmonic Acid and Represses Basal Defense and Resistance Responses against Botrytis cinerea Infection. Mol. Plant 10, 1159–1173. https://doi.org/10.1016/j.molp.2017.07.010

Sørensen, J.L., Benfield, A.H., Wollenberg, R.D., Westphal, K., Wimmer, R., Nielsen, M.R., Nielsen, K.F., Carere, J., Covarelli, L., Beccari, G., Powell, J., Yamashino, T., Kogler, H., Sondergaard, T.E., Gardiner, D.M., 2018. The cereal pathogen Fusarium pseudograminearum produces a new class of active cytokinins during infection. Mol. Plant Pathol. 19, 1140–1154. https://doi.org/10.1111/mpp.12593

Spallek, T., Gan, P., Kadota, Y., Shirasu, K., 2018. Same tune, different song — cytokinins

as virulence factors in plant–pathogen interactions? Curr. Opin. Plant Biol. 44, 82–87. https://doi.org/10.1016/j.pbi.2018.03.002

Spence, C.A., Lakshmanan, V., Donofrio, N., Bais, H.P., 2015. Crucial roles of abscisic acid biogenesis in virulence of rice blast fungus Magnaporthe oryzae. Front. Plant Sci. 6, 1–13. https://doi.org/10.3389/fpls.2015.01082

Sperschneider, J., Dodds, P.N., Gardiner, D.M., Singh, K.B., Taylor, J.M., 2018. Improved prediction of fungal effector proteins from secretomes with EffectorP 2.0. Mol. Plant Pathol. 19, 2094–2110. https://doi.org/10.1111/mpp.12682

Sperschneider, J., Gardiner, D.M., Thatcher, L.F., Lyons, R., Singh, K.B., Manners, J.M., Taylor, J.M., 2015. Genome-wide analysis in three Fusarium pathogens identifies rapidly evolving chromosomes and genes associated with pathogenicity. Genome Biol. Evol. 7, 1613–1627. https://doi.org/10.1093/gbe/evv092

Stephens, A.E., Gardiner, D.M., White, R.G., Munn, A.L., Manners, J.M., 2008. Phases of infection and gene expression of Fusarium graminearum during crown rot disease of wheat. Mol. Plant-Microbe Interact. 21, 1571–1581. https://doi.org/10.1094/MPMI-21-12-1571

Strange, R., Smith, H., Majer, J., 1972. Choline, One of Two Fungal Growth Stimulants in Anthers responsible for the Susceptibility of Wheat to Fusarium graminearum. Nature 238, 103–104. https://doi.org/10.1038/238103a0

Struck, C., 2015. Amino acid uptake in rust fungi. Front. Plant Sci. 6, 1–6. https://doi.org/10.3389/fpls.2015.00040

Svoboda, T., Parich, A., Güldener, U., Schöfbeck, D., Twaruschek, K., Václavíková, M., Hellinger, R., Wiesenberger, G., Schuhmacher, R., Adam, G., 2019. Biochemical Characterization of the Fusarium graminearum Candidate ACC-Deaminases and Virulence Testing of Knockout Mutant Strains. Front. Plant Sci. 10, 1–17.

https://doi.org/10.3389/fpls.2019.01072

Torrens-Spence, M.P., Bobokalonova, A., Carballo, V., Glinkerman, C.M., Pluskal, T., Shen, A., Weng, J.-K., 2019. PBS3 and EPS1 complete salicylic acid biosynthesis from isochorismate in Arabidopsis. bioRxiv 601948. https://doi.org/10.1101/601948

Trail, F., 2009. For Blighted Waves of Grain: Fusarium graminearum in the Postgenomics Era: Figure 1. Plant Physiol. 149, 103–110. https://doi.org/10.1104/pp.108.129684

Tsitsigiannis, D.I., Keller, N.P., 2007. Oxylipins as developmental and host-fungal communication signals. Trends Microbiol. 15, 109–118. https://doi.org/10.1016/j.tim.2007.01.005

Ursache, R., Andersen, T.G., Marhavý, P., Geldner, N., 2018. A protocol for combining fluorescent proteins with histological stains for diverse cell wall components. Plant J. 93, 399–412. https://doi.org/10.1111/tpj.13784

Voigt, C.A., Schäfer, W., Salomon, S., 2005. A secreted lipase of Fusarium graminearum is a virulence factor required for infection of cereals. Plant J. 42, 364–375. https://doi.org/10.1111/j.1365-313X.2005.02377.x

Wang, H., Sun, S., Ge, W., Zhao, L., Hou, B., Wang, K., Lyu, Z., Chen, L., Xu, S., Guo, J., Li, M., Su, P., Li, Xuefeng, Wang, G., Bo, C., Fang, X., Zhuang, W., Cheng, X., Wu, J., Dong, L., Chen, W., Li, W., Xiao, G., Zhao, J., Hao, Y., Xu, Y., Gao, Y., Liu, W., Liu, Y., Yin, H., Li, J., Li, Xiang, Zhao, Y., Wang, X., Ni, F., Ma, X., Li, A., Xu, S.S., Bai, G., Nevo, E., Gao, C., Ohm, H., Kong, L., 2020. Horizontal gene transfer of Fhb7 from fungus underlies Fusarium head blight resistance in wheat. Science (80-.). 5435, eaba5435. https://doi.org/10.1126/science.aba5435

Wang, L., Li, Q., Liu, Z., Surendra, A., Pan, Y., Li, Y., Zaharia, L.I., Ouellet, T., Fobert, P.R., 2018. Integrated transcriptome and hormone profiling highlight the role of multiple phytohormone pathways in wheat resistance against fusarium head blight. PLoS One

13, e0207036. https://doi.org/10.1371/journal.pone.0207036

Wang, Q., Shao, B., Shaikh, F.I., Friedt, W., Gottwald, S., 2018. Wheat Resistances to Fusarium Root Rot and Head Blight Are Both Associated with Deoxynivalenol- and Jasmonate-Related Gene Expression. Phytopathology 108, 602–616. https://doi.org/10.1094/PHYTO-05-17-0172-R

Wang, Q., Vera Buxa, S., Furch, A., Friedt, W., Gottwald, S., 2015. Insights Into *Triticum aestivum* Seedling Root Rot Caused by *Fusarium graminearum*. Mol. Plant-Microbe Interact. 28, 1288–1303. https://doi.org/10.1094/MPMI-07-15-0144-R

Wiemann, P., Sieber, C.M.K., von Bargen, K.W., Studt, L., Niehaus, E.M., Espino, J.J., Huß, K., Michielse, C.B., Albermann, S., Wagner, D., Bergner, S. V., Connolly, L.R., Fischer, A., Reuter, G., Kleigrewe, K., Bald, T., Wingfield, B.D., Ophir, R., Freeman, S., Hippler, M., Smith, K.M., Brown, D.W., Proctor, R.H., Münsterkötter, M., Freitag, M., Humpf, H.U., Güldener, U., Tudzynski, B., 2013. Deciphering the Cryptic Genome: Genome-wide Analyses of the Rice Pathogen Fusarium fujikuroi Reveal Complex Regulation of Secondary Metabolism and Novel Metabolites. PLoS Pathog. 9. https://doi.org/10.1371/journal.ppat.1003475

Wildermuth, M.C., Dewdney, J., Wu, G., Ausubel, F.M., 2002. Isochorismate synthase is required to synthesize salicylic acid for plant defence. Nature 417, 571–571. https://doi.org/10.1038/417571a

Yan, X., Talbot, N.J., 2016. Investigating the cell biology of plant infection by the rice blast fungus Magnaporthe oryzae. Curr. Opin. Microbiol. 34, 147–153. https://doi.org/10.1016/j.mib.2016.10.001

Yang, F., Jensen, J.D., Svensson, B., Jørgensen, H.J.L., Collinge, D.B., Finnie, C., 2012. Secretomics identifies Fusarium graminearum proteins involved in the interaction with barley and wheat. Mol. Plant Pathol. 13, 445–453. https://doi.org/10.1111/j.1364-3703.2011.00759.x

1171 Yin, Y., Wang, Z., Cheng, D., Chen, X., Chen, Y., Ma, Z., 2018. The ATP-binding protein
1172 FgArb1 is essential for penetration, infectious and normal growth of Fusarium
1173 graminearum. New Phytol. 219, 1447–1466. https://doi.org/10.1111/nph.15261

1174 Yu, J.H., Wieser, J., Adams, T.H., 1996. The Aspergillus FlbA RGS domain protein
1175 antagonizes G protein signaling to block proliferation and allow development. EMBO J.
1176 15, 5184–5190. https://doi.org/10.1002/j.1460-2075.1996.tb00903.x

1177 Yu, Y., Ouyang, Y., Yao, W., 2018. ShinyCircos: An R/Shiny application for interactive
1178 creation of Circos plot. Bioinformatics 34, 1229–1231.
1179 https://doi.org/10.1093/bioinformatics/btx763

1180 Zhang, X.-W., Jia, L.-J., Zhang, Y., Jiang, G., Li, X., Zhang, D., Tang, W.-H., 2012. In Planta
1181 Stage-Specific Fungal Gene Profiling Elucidates the Molecular Strategies of Fusarium
1182 graminearum Growing inside Wheat Coleoptiles. Plant Cell 24, 5159–5176.
1183 https://doi.org/10.1105/tpc.112.105957

1184 Zhang, Y., He, J., Jia, L.J., Yuan, T.L., Zhang, D., Guo, Y., Wang, Y., Tang, W.H., 2016.
1185 Cellular Tracking and Gene Profiling of Fusarium graminearum during Maize Stalk Rot
1186 Disease Development Elucidates Its Strategies in Confronting Phosphorus Limitation in
1187 the Host Apoplast. PLoS Pathog. 12, 1–33.
1188 https://doi.org/10.1371/journal.ppat.1005485

1189 Zhou, S., Zhang, Y.K., Kremling, K.A., Ding, Y., Bennett, J.S., Bae, J.S., Kim, D.K.,
1190 Ackerman, H.H., Kolomiets, M. V., Schmelz, E.A., Schroeder, F.C., Buckler, E.S.,
1191 Jander, G., 2019. Ethylene signaling regulates natural variation in the abundance of
1192 antifungal acetylated diferuloylsucroses and Fusarium graminearum resistance in
1193 maize seedling roots. New Phytol. 221, 2096–2111. https://doi.org/10.1111/nph.15520

1194

1195 **Figures**

Figure 1. Global regulation of *Fg* genes during *Bd* root colonization. (A) Expression of 2049 *Fg* genes that were differentially regulated during *Bd* root infections (*Fg-Bd*) relative to *Fg* grown in culture (*Fg*-only). Proteins encoded by differentially expressed genes (DEGs) are assigned to four functional categories as shown in the right side of the figure. (B) Key features of 225 DEGs associated with carbohydrate active enzymes (CAZymes). Enzymatic functions and substrate specificities were predicted as shown in the right side of the figure. PCW: plant cell wall, FCW: fungal cell wall. (C) Key features of 251 DEGs encoding putative secreted proteins. *Bd* roots colonized by *Fg* (*Fg-Bd*) were harvested at 5 dpi and *Fg* mycelia grown without *Bd* roots were used as control (*Fg*-only). Transcript levels of fungal genes were presented as normalized FPKM (Fragments Per Kilobase of transcript per Million mapped reads) values and log2-transformed. Heatmap colour range represents high to low expression levels. The dendrogram shows distance similarity of expression of each gene.

Figure 2. The number of *Fg* genes upregulated during *Bd* root infection were also induced or actively expressed during the infection of other tissues by *Fg*, suggesting that a core number of *Fg* genes could be broadly associated with infection (A) The Venn diagram showing how many *Fg* genes that were observed to be up-regulated during *Bd* root infection in this study were common to those upregulated or differentially expressed in different tissues of wheat (*Triticum aestivum*, *Ta*), barley (*Hordeum vulgare, Hv*) and maize (*Zea mays*, *Zm*). (B) The heatmap showing differential expression profiles of 38 core *Fg* genes identified from (A) between *in vitro* growth and during *Bd* root infection. FPKM values from three independent biological replicates were log2-transformed. Putative proteins encoded by these genes are shown on the right.

Figure 3. Genome-wide comparison of *Fg* and *F. pseudograminearum* (*Fp*) gene expression patterns during infection of *Bd* roots (this study) and aboveground tissues (Powell et al., 2017). (**A**) Chromosomal locations and syntenic relationship of highly conserved *Fg* and *Fp* genes. (1-4: *Fg* chromosomes; NC_031952.1-NC_031952.4: *Fp* chromosomes). (**B**) The top 20 genes with the most contrasted expression values were selected from chromosome 2 of

Fg and *Fp* genomes, respectively. Heat maps in A and B display expression of genes as log2-transformed FPKM values from three biological replicates. Colour range is indicated as high (red) to low (blue).

Figure 4. Global regulation of *Fg* genes in the *Tri5* mutant during *Bd* root colonization. (A) Expression of 974 *Fg* genes that were differentially expressed WT *Fg* and ΔTri5 during *Bd* root infection. Proteins encoded by DEGs were assigned to four functional categories as shown on the right. (B) Key features of 95 DEGs associated with carbohydrate active enzymes (CAZymes). Plant cell wall (PCW) degradation functions and substrate specificities were predicted as shown in the right-hand side. (C) Key features of 124 DEGs encoding putative secreted proteins. *Bd* roots inoculated with *Fg* WT and ΔTri5 strains were harvested at 5 dpi for the RNA-seq analysis. Transcript levels of *Fg* genes were log2-transformed and presented as normalized FPKM values. Heatmap colour range representing high to low expression levels is shown. Dendrograms show distance similarity of expression of each gene.

Figure 5. Lignin deposition in response to *Fg* infection is reduced in *Bd* roots inoculated with ΔTri5. *Bd* roots either mock-treated or inoculated with either WT *Fg* or ΔTri5 were harvested at 5 dpi. Red fluorescence signals (lower panels) indicate lignin deposition stained by Basic Fuchsin. Shown are representatives of at least 6 independent roots from three biological replicates. Images were taken using 561nm excitation and detected at 600–650 nm on a Zeiss Axio Imager M2 microscopy.

Figure 6. Quantification of selected phytohormones and DON in *Bd* roots inoculated with either WT *Fg* or the ΔTri5 mutant; jasmonic acid (JA) (**A**), methyl-jasmonate (MeJA) (**B**), salicylic acid (SA) (**C**), deoxynivalenol (DON) (**D**), indole-3-acetic acid (IAA) (**E**) and gibberellic acid (GA) (**F**) analysed by high-performance liquid chromatography. Independently grown fungal mycelium on minimal media (MM) (*Fg*-only), uninoculated *Bd* roots (*Bd*-only), as well as *Bd* roots inoculated with WT *Fg* or ΔTri5 infected roots were collected from MM at 5 dpi and subjected to metabolite extraction. Pure MM was used as

background control. Metabolite quantifications were conducted according to the concentration-gradient derived standard curves of JA, MeJA, SA, DON, IAA and GA. Error bars indicate standard error of the mean based on six biological replicates, each comprising of 10 plants or 1 plate of fungal mycelium. Asterisks represent differences that were statistically significant (unpaired two-tailed t-test, *P< 0.05. ****P< 0.0001).

Figure 7. Deoxynivalenol (DON) produced by *F. graminearum* (*Fg*) during the infection of *B. distachyon* (*Bd*) roots does not contribute to lesion formation. Microscopic pictures were taken for *Bd* roots colonized by *Fg* strains after two days post inoculation (dpi). (**A**) DON is produced during the infection of *Bd* roots by *Fg*. Strong florescence signals could be observed in the mycelium of a *Fg* strain expressing a *Tri5-GFP* fusion construct driven by the native *Tri5* promoter. (**B**) No GFP signals could be detectable for WT *Fg* during root infection. **(C)** Transcriptional activation of *Tri5* confirms DON production in infected roots. Expressions of *Tri5*, *Flp1,* a lipase encoding gene previously identified as a virulence factor in *Fg* and a *Bd* ubiquitin-conjugating enzyme 18 gene (*UBC18*) used for fungal biomass measurements were quantified by RT-qPCR relative to the fungal *α-tubulin.* Root samples were harvested at 2, 3, 4, 5, and 7 dpi from three independent biological replicates each with at least 12 individual plants. (**D**) Deoxynivalenol (DON) does not contribute to lesion formation in *Bd* roots. Representative photos showing colonization of *Bd* roots with the WT *Fg* and *Tri5* deletion mutants.

Figure 8. SA hydroxylase-like genes present in the *Fg* genome and their expression profiles during growth in culture or infection of *Bd* roots. (**A**) Phylogenetic unrooted tree of SA hydroxylase protein homologs of NahG, Arabidopsis Dlo1 (AT4G10500) and Dmr6 (AT5G24530) in *Fg*. The protein evolutionary models were tested using Neighbor-Joining inference and then referred to tree building based on Maximum Likelihood method. (**B**) Expressions of 28 SA hydroxylase candidate genes during *Bd* root infections or *in vitro* growth on minimal medium (MM). Heatmap shows expression levels of each gene displayed as log-transformed FPKM values of three replicates from low (blue) to high (red). *Fg* genes

significantly induced during *Bd* root infection were marked as 'yes'. An overview of concatenated alignment of all protein sequences was shown aside.

A

Expression log_2(FPKM+0.01)

-4<

> 4

Fg-only

Fg-Bd

SM enzyme

Secreted

CAzyme

Transporter

B

CAZymes

Hemicellulose

Pectin

Lignin

Hemicellulose_or_pectin_side_chains

Cellulose

Fg-only

Fg-Bd

225

PCW

FCW

PCW or FCW

Substrate

C

Secreted proteins

Fg-only

Fg-Bd

251

CAZyme

Effector

Lipase

Protease

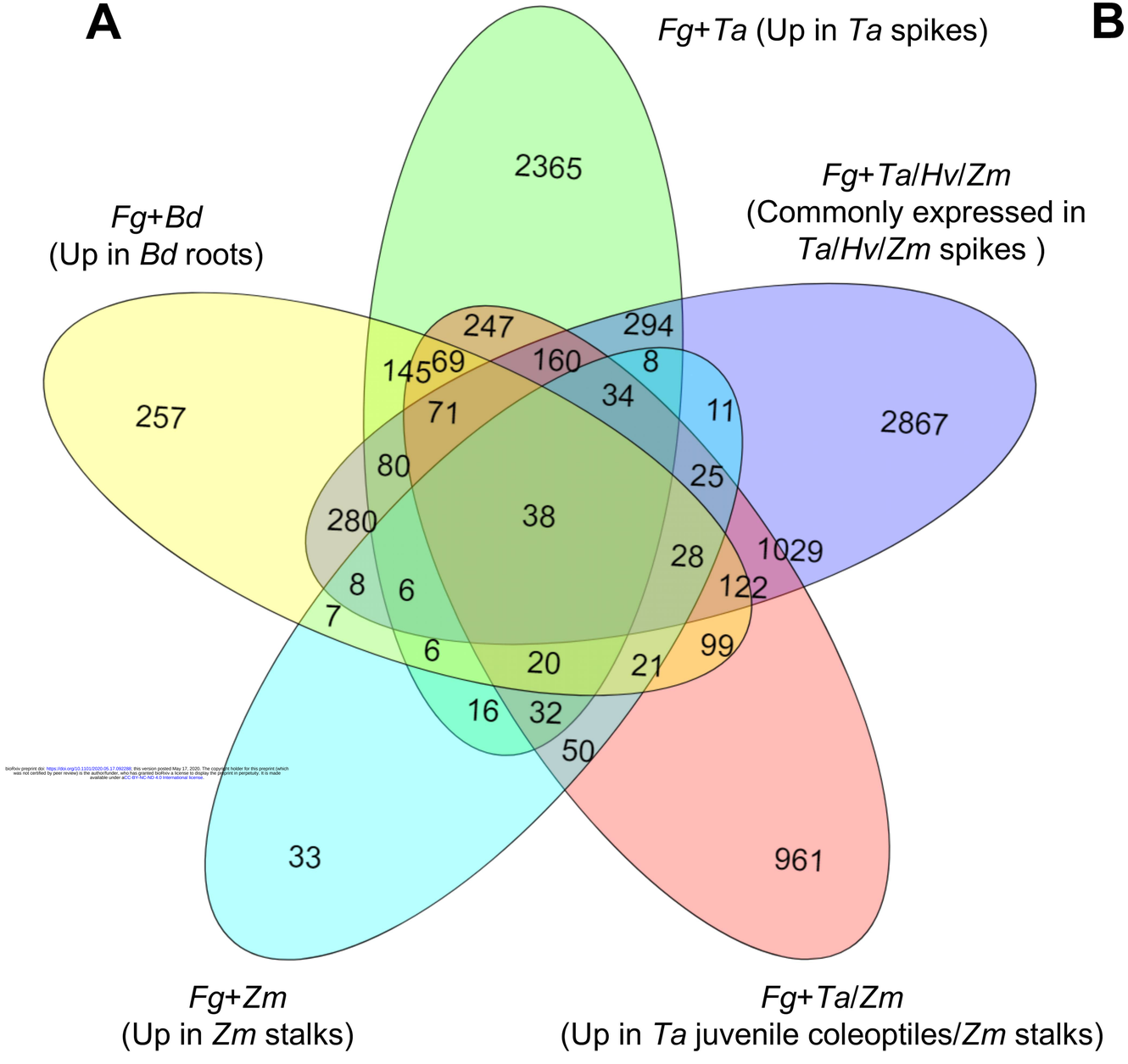

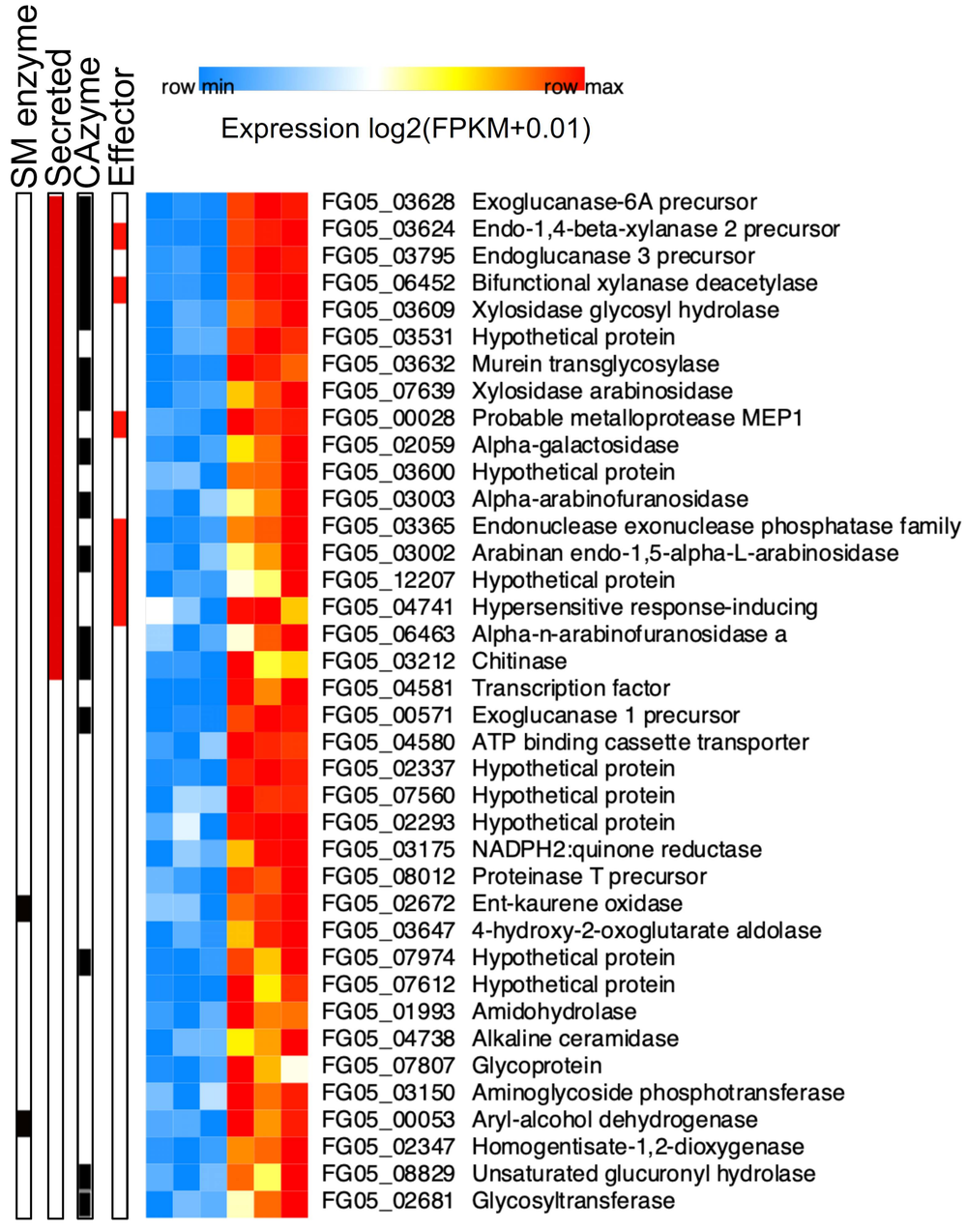

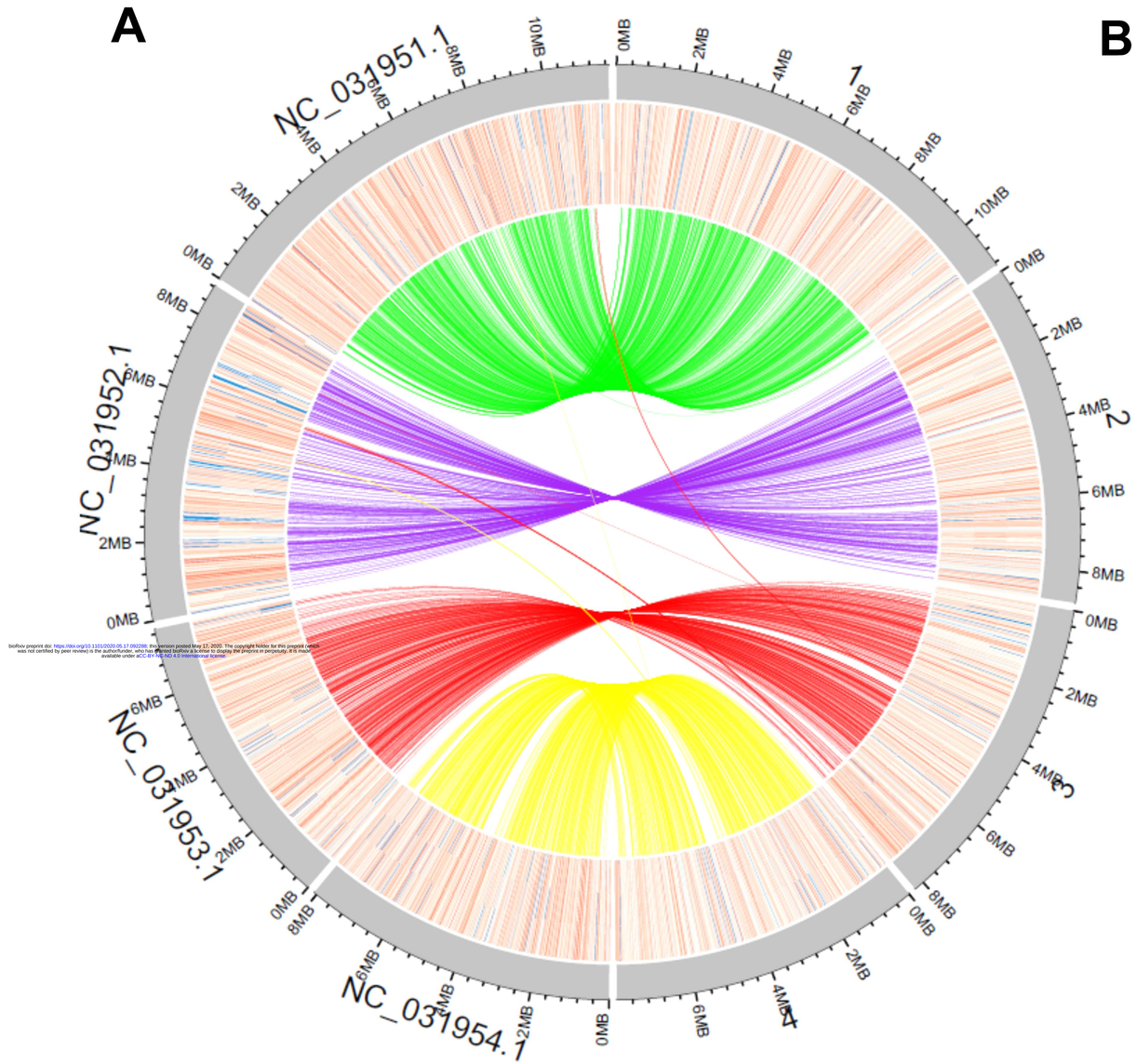

B

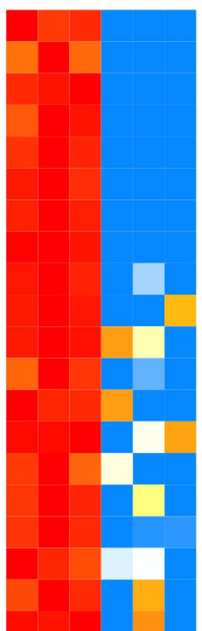

Fg Gene ID	Fp GeneID	Annotation
FG05_03352	FPSE_04684	Related to cell wall glycoprotein (SP)
FG05_08075	FPSE_07536	Astacin-domain contaning metallopeptidase
FG05_03387	FPSE_10631	Probablelbeta-glucosidase (SP)
FG05_03727	FPSE_06095	Zn_2Cys_6 transcription factor
FG05_02880	FPSE_06666	Molybdopterin oxidoreductase
FG05_04644	FPSE_08103	Putative MFS-type transporter
FG05_03732	FPSE_06100	Putative MFS-type transporter
FG05_08493	FPSE_04628	Putative secreted (SP)
FG05_08141	FPSE_05463	Probable glutamate carboxypeptidase (SP)
FG05_08265	FPSE_09545	Probable glucan endo-1,6-beta-glucosidase (SP)
FG05_03728	FPSE_06096	Phytanoyl-CoA dioxygenase
FG05_03083	FPSE_02142	Sugar MFS-type transporter
FG05_02968	FPSE_06765	GPR1/FUN34/YaaH-class plasma membrane protein
FG05_08396	FPSE_09013	N-acetylglucosamine-6-phosphate deacetylase
FG05_03914	FPSE_05362	Isochorismatase-like (SP)
FG05_03726	FPSE_06094	Putative MFS-type transporter
FG05_08077	FPSE_07534	NADH-flavin oxidoreductase
FG05_04458	FPSE_09906	Probable flavohemoglobin
FG05_13388	FPSE_09464	TauD domain-containing oxidoreductase
FG05_04355	FPSE_12089	Cyclin domain-containing protein

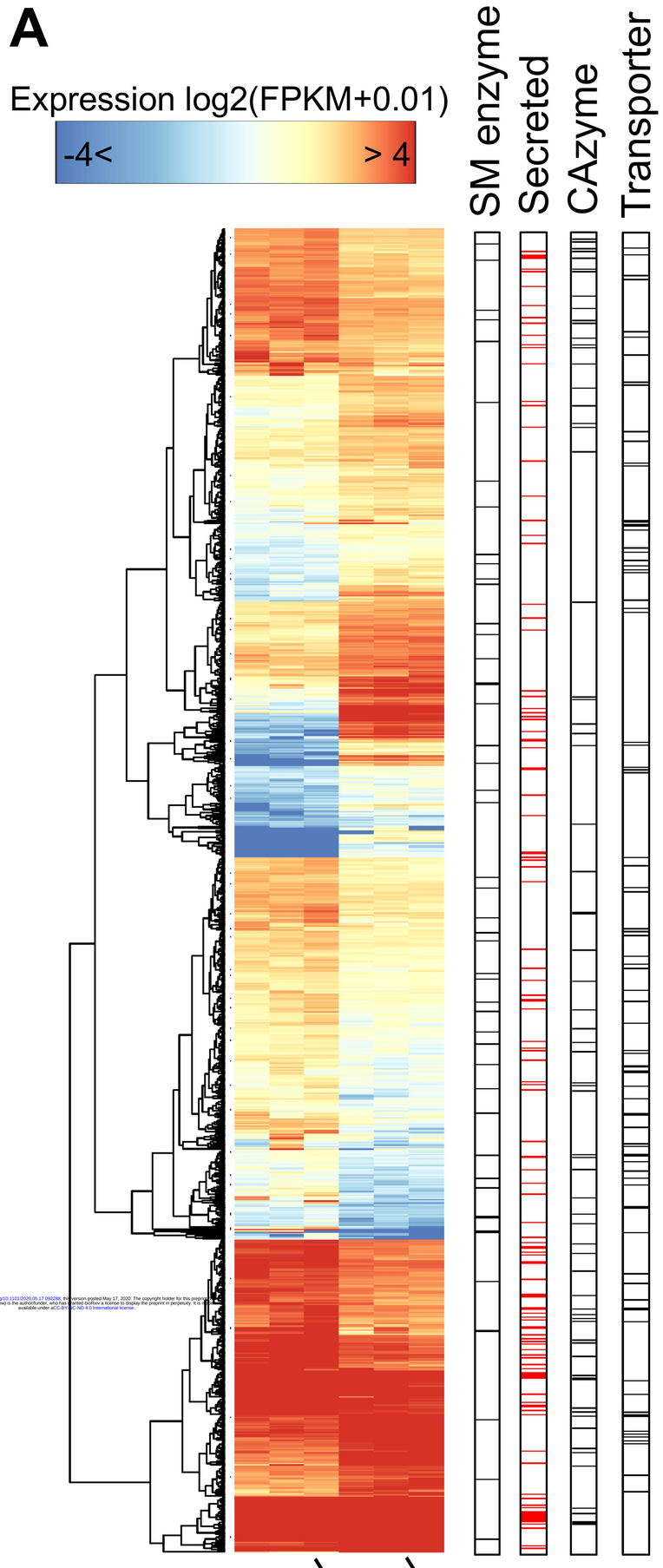

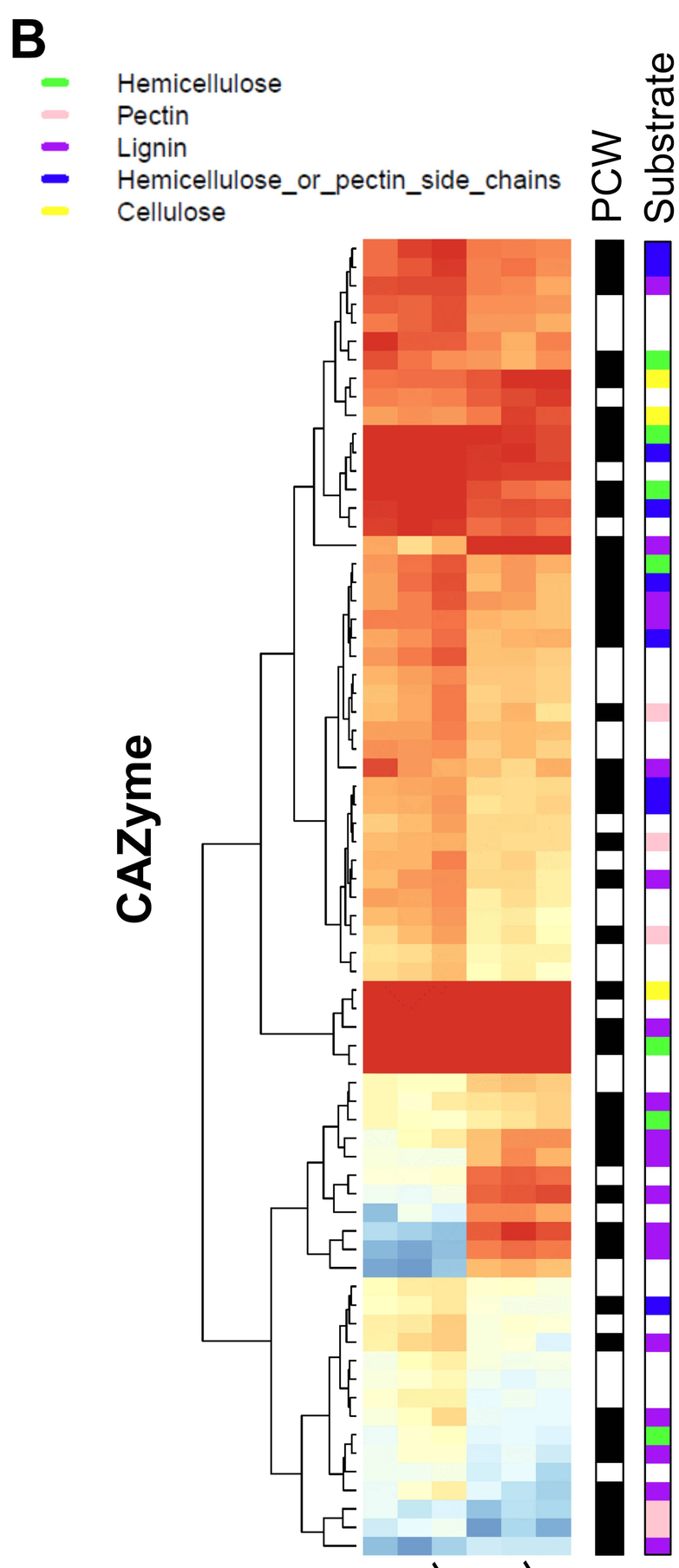

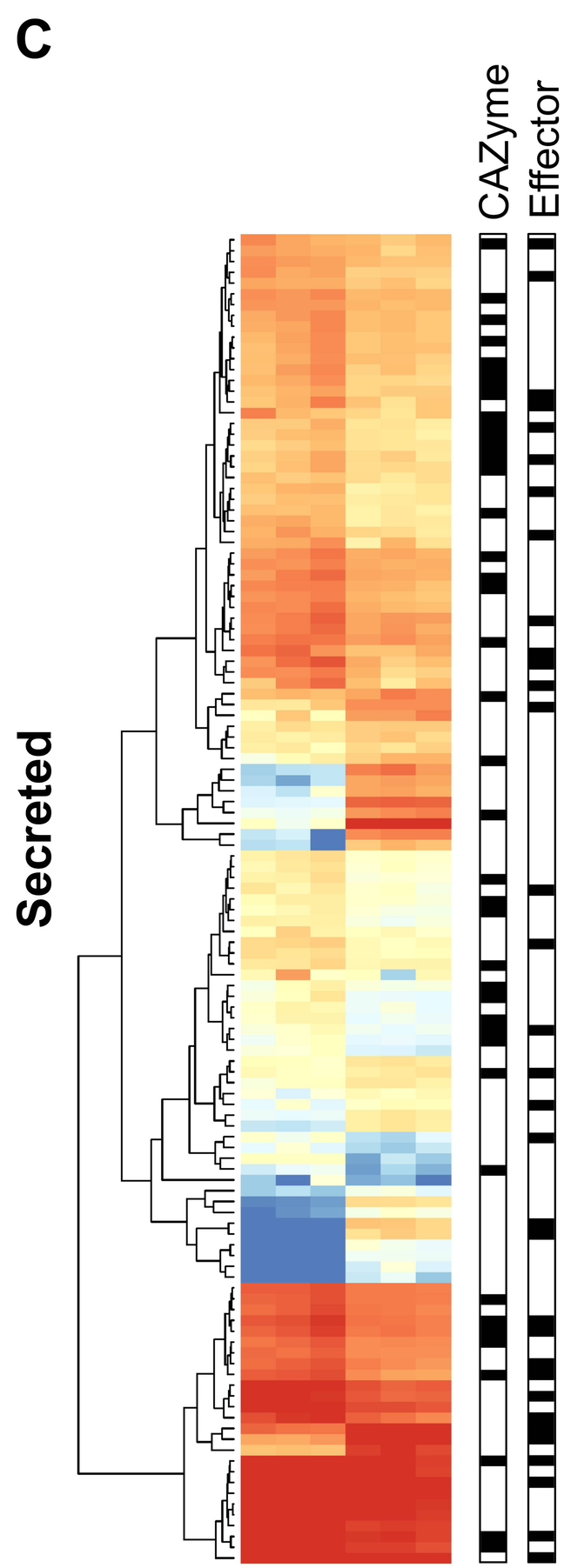

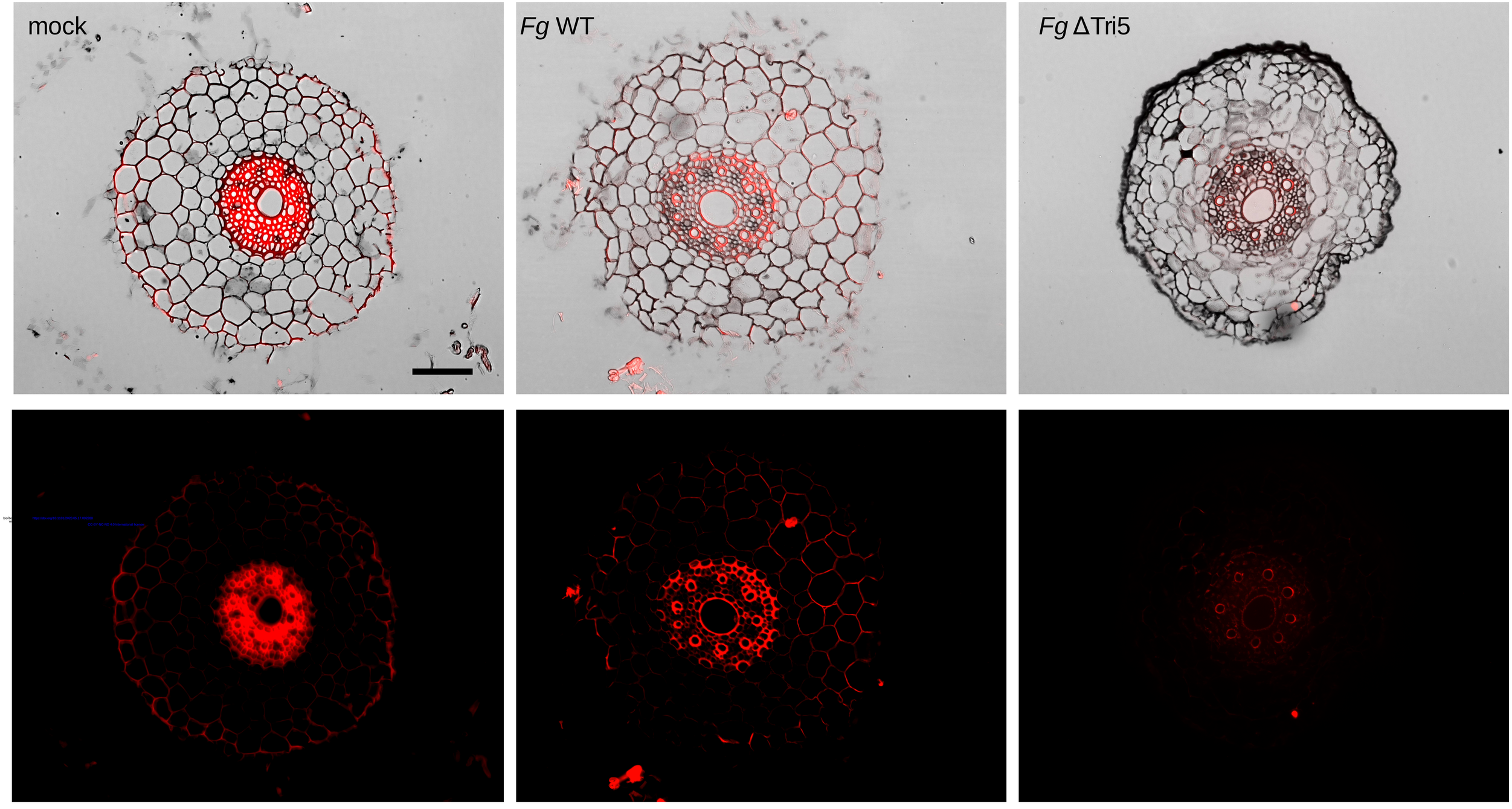
mock
Fg WT
Fg ΔTri5

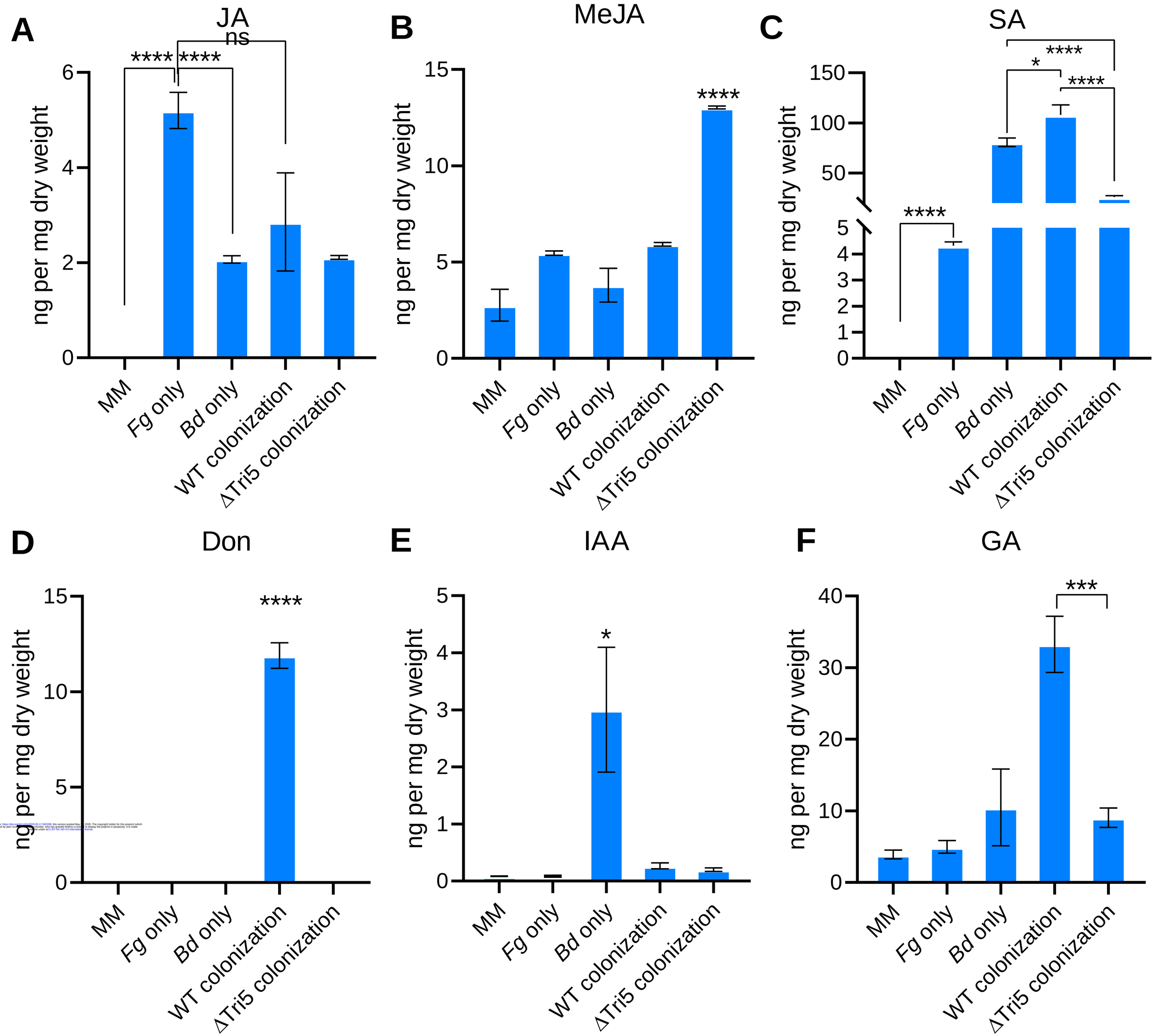

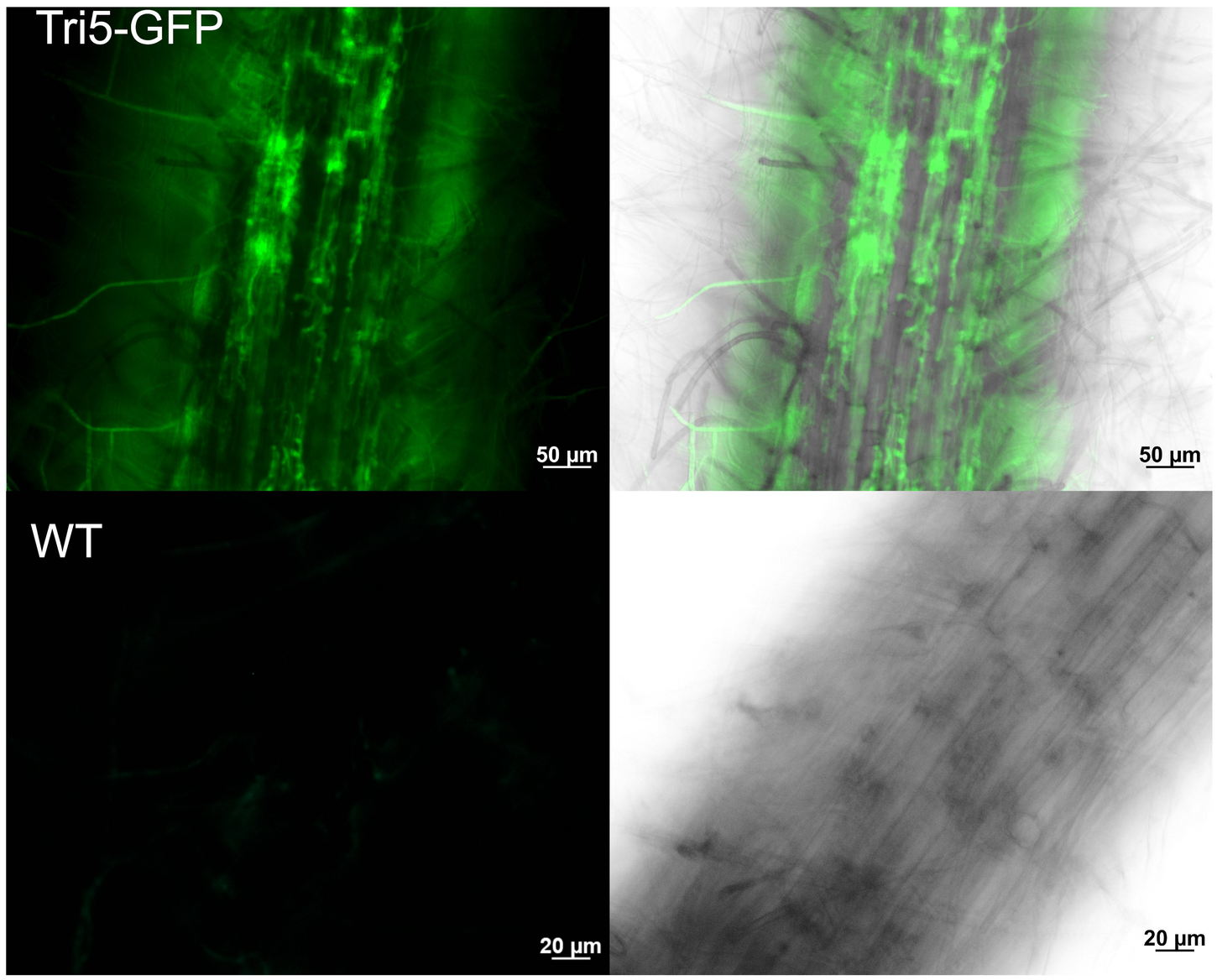

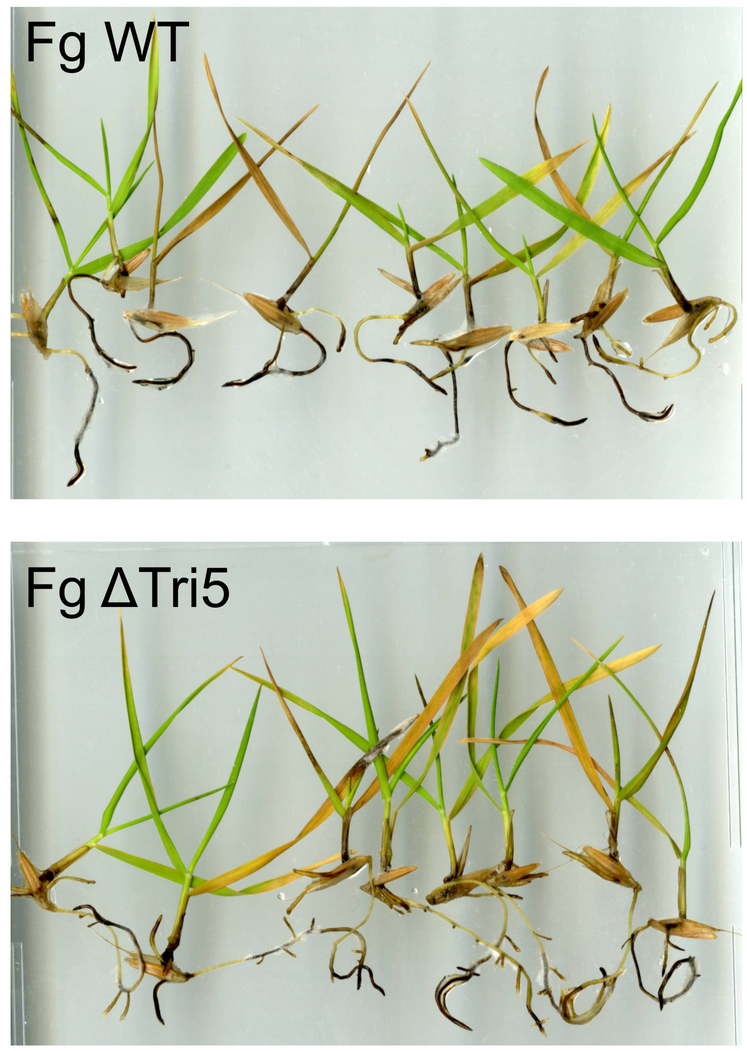

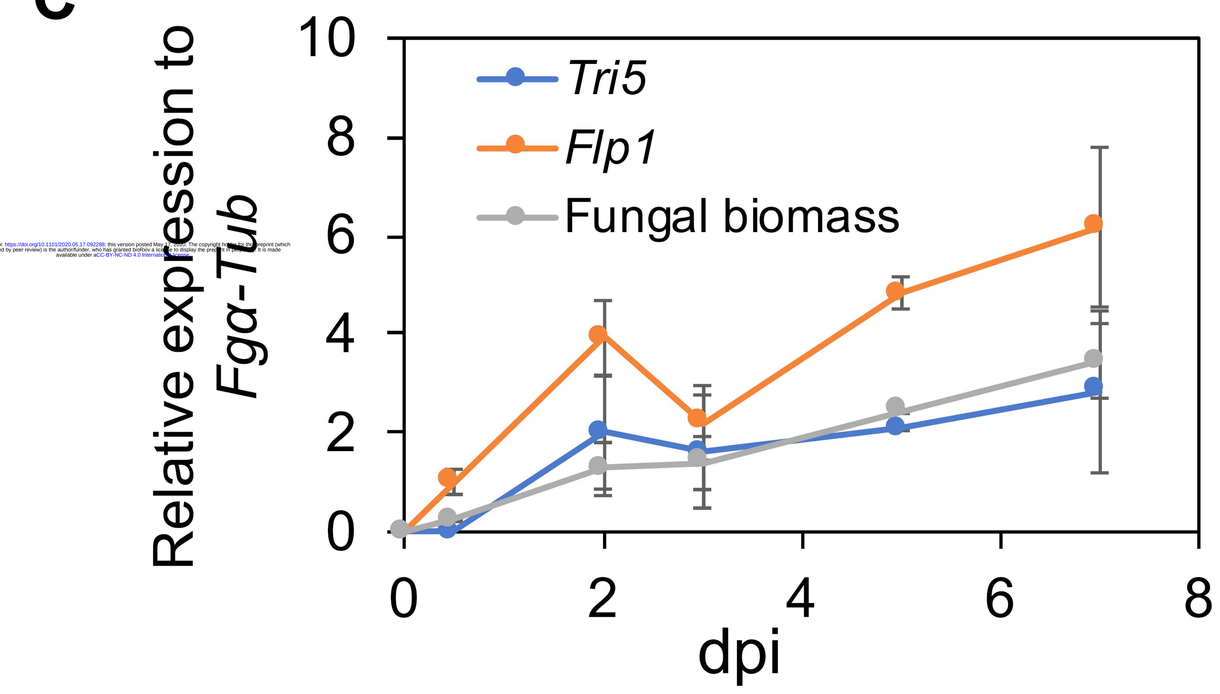

A

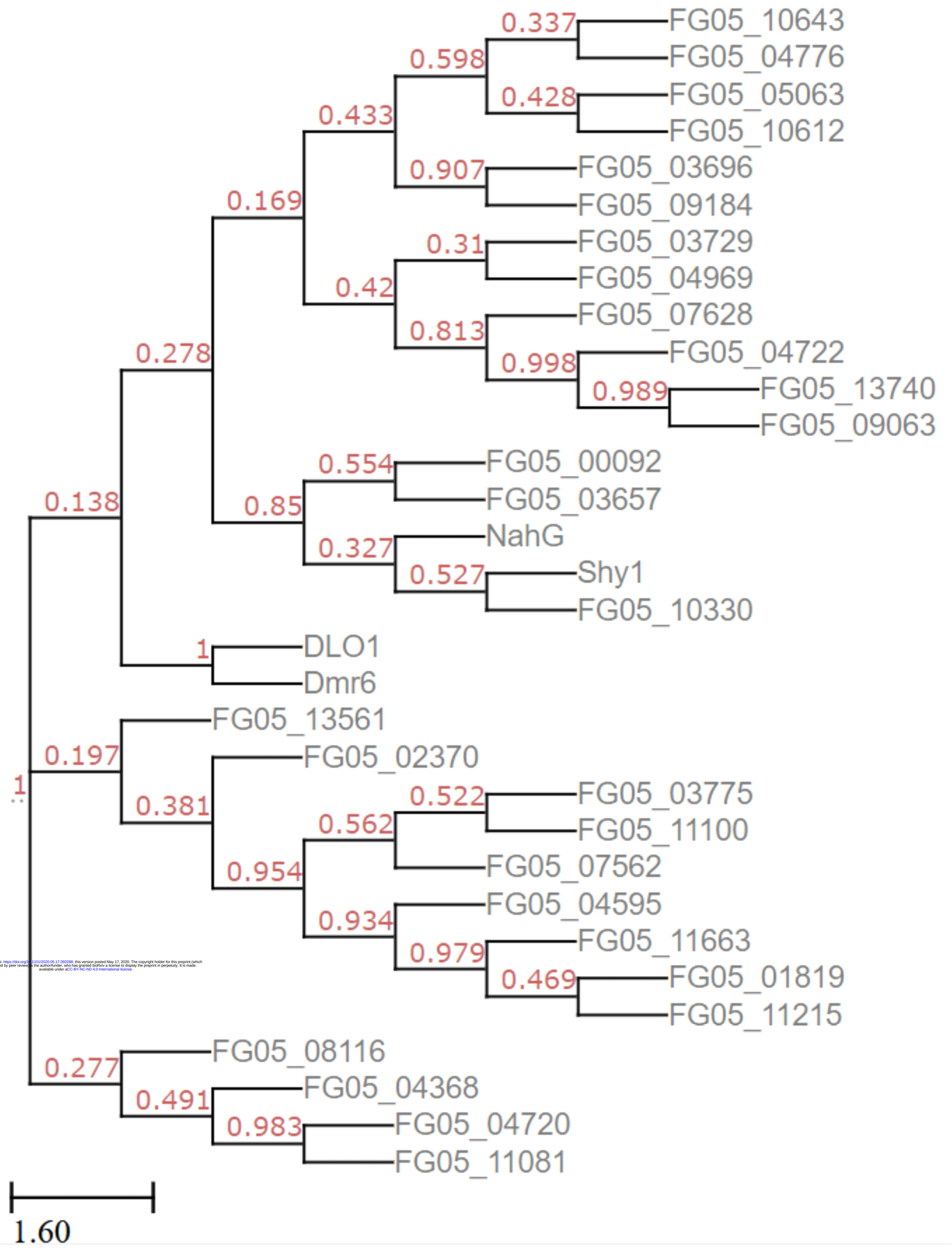

B